

Single Photon-Evoked Events of the Ventral Nerve Photoreceptor Cell of *Limulus*

Facilitation, Adaptation and Dependence of Lowered External Calcium

H. Stieve, H. Reuß, H. T. Hennig, and J. Klomfaß

Institut für Biologie II RWTH Aachen, Kopernikusstraße 16, D-5100 Aachen, Bundesrepublik Deutschland

Z. Naturforsch. **46c**, 461–486 (1991); received December 7, 1990

Limulus Photoreceptor, Quantum Bumps, Linear Bump Sum, Adaptation, Facilitation, Calcium, Magnesium

Bumps, the elementary excitatory events of the *Limulus* ventral nerve photoreceptor following a weak flash of light were recorded under voltage clamp conditions. The statistical distribution of various bump parameters and their changes caused by weak conditioning pre-illumination are described, and the influence of lowered external Ca^{2+} -concentration together with normal or raised Mg^{2+} -concentration (15 °C).

1) *Weak conditioning pre-illumination* causes desensitization: the bump current amplitude, bump duration, bump area (current-integral), and the bump latency are diminished, the more, the stronger the conditioning flash, *i.e.* the light adaptation.

Very weak conditioning pre-illumination causes *facilitation*, expressed by an increase in number and size of the observed bumps. The average bump latency, however, is already shortened under these conditions.

2) *Lowering the external Ca^{2+} -concentration* from 10 mmol/l to 250 $\mu\text{mol/l}$ has its primary effect on the dark-adapted photoreceptor (without substantially reducing the ability for light-adaptation). It causes the following average changes: the amplitudes, durations, current-integrals, and the latencies of current bumps are greatly enlarged and the number of bumps is raised.

3) Raised magnesium concentration from 50 to 100 mmol/l can partially compensate for the lack of calcium; however, it enhances the effect of calcium deficiency on the latency, *i.e.* it further enlarges the average latencies.

The results can be explained on the basis of our model of bump generation by two assumptions.

1) Lowering the external calcium concentration causes a decrease in the cytosolic Ca^{2+} -level without substantially reducing the intracellular calcium stores from which the light-adapting calcium release is fed. The lowered cytosolic Ca^{2+} -concentration induces an “extra” dark adaptation resulting in greater bumps and more bumps exceeding the threshold of recognition. The bump latency, however, which behaves differently from all other bump parameters, is determined by a separate calcium-dependent reaction where magnesium competes with calcium antagonistically.

2) Facilitation is due to cooperativity of transmitter binding in order to open the ion channels.

Introduction

When the *Limulus* photoreceptor is bathed in physiological saline the successful absorption of a

photon by a rhodopsin molecule starts a sequence of reactions which lead to the generation of a relatively large elementary excitatory response, the

Abbreviations: A [nA], peak amplitude of receptor current; cAMP, adenosine 3':5'-cyclic monophosphate; cGMP, guanosine 3':5'-cyclic monophosphate; CH, ion channel in membrane; E_c [photons/cm²], energy of conditioning illumination; E_w [photons/cm²], energy of response-evoking flash; F [pC = nA·ms], area, current-integral of light-induced membrane current; IBMX, 3-isobutyl-1-methylxanthine; IP₃, inositol 1,4,5-trisphosphate; J_{max} [nA], peak amplitude of bump sum; m [nA/ms], average slope A/TR of signal rise; $N + \text{NR}$, number of single and riding bumps; N , number of evaluable single bumps; N_b , total number of bumps = $N + \text{NR}$; N_s , number of stimuli; PS, physiological saline; Q, source of transmitter or messenger; ReC [nA], receptor current,

membrane current signal in response to light stimulus; ReP [mV], receptor potential, light-evoked voltage signal; SRC, subrhabdomic cisternae; T, intracellular transmitter or messenger in phototransduction; TA [ms], time-to-peak of bump from stimulus onset; TB [ms], bump duration; TLAT [ms], latent period, time from stimulus onset until first measurable increase of response; TMAX [ms], time-to-peak from stimulus onset for bump sum; TR [ms], time of rise, TA – TLAT.

Reprint requests to Prof. H. Stieve.

Verlag der Zeitschrift für Naturforschung, D-7400 Tübingen
0939–5075/91/0500–0461 \$ 01.30/0



Dieses Werk wurde im Jahr 2013 vom Verlag Zeitschrift für Naturforschung in Zusammenarbeit mit der Max-Planck-Gesellschaft zur Förderung der Wissenschaften e.V. digitalisiert und unter folgender Lizenz veröffentlicht: Creative Commons Namensnennung-Keine Bearbeitung 3.0 Deutschland Lizenz.

Zum 01.01.2015 ist eine Anpassung der Lizenzbedingungen (Entfall der Creative Commons Lizenzbedingung „Keine Bearbeitung“) beabsichtigt, um eine Nachnutzung auch im Rahmen zukünftiger wissenschaftlicher Nutzungsformen zu ermöglichen.

This work has been digitalized and published in 2013 by Verlag Zeitschrift für Naturforschung in cooperation with the Max Planck Society for the Advancement of Science under a Creative Commons Attribution-NoDerivs 3.0 Germany License.

On 01.01.2015 it is planned to change the License Conditions (the removal of the Creative Commons License condition “no derivative works”). This is to allow reuse in the area of future scientific usage.

“bump”. The conclusion that light-evoked bumps are single photon-evoked events follows from the statistical noise analysis of the number of bumps evoked by dim flashes [1–3] and from the bump interval distribution [4]. A bump is a transient increase of the cation conductance of the visual cell membrane and follows photon absorption after a long (on the average 300 ms, but occasionally up to more than 1 s) and greatly variable delay. The bump size also varies greatly, indicating the variation in the degree of amplification in the transduction process. A bump is believed to be composed of a volley of a large number of transiently opened ion-specific channels through the cell membrane.

A large bump of a dark-adapted *Limulus* photoreceptor involves a cation conductance increase of about 10 to 20 nS in the bump maximum. One can estimate that in the maximum of a large bump up to 10^3 ion channels with a single channel conductance of 10 to 40 pS (10–20 pS [5]; 40 pS [6, 8]; 10 and 30 pS [9, 10]) are opened simultaneously. Since the mean open time of the channels is short (1.5 or 5.5 ms [10]) compared to the bump duration a large bump probably consists of a volley of more than 10^4 poorly synchronized single channel openings. Bump generation thus involves a large, variable amplification – considering the number of ion channels opened in consequence of the light-activation of a single rhodopsin molecule as measure of amplification.

Bumps are observed even after the *Limulus* photoreceptor cell has stayed in the dark for hours after its last stimulation. The question arises whether these “bumps in the dark” are light-evoked with extremely large delay or whether they are generated spontaneously: The strong temperature dependence of the frequency of the observed “dark bumps” [11, 12] indicates that the bumps observed after longer stays in the dark are triggered by a thermally activated reaction, most probably by the back reaction from inactivated metarhodopsin to the activated state [13, 14]. As observed by Yeandle and Spiegler [15], Goldring and Lisman [16] and Stieve and Bruns [17], the average amplitude of light-evoked bumps is larger than that of bumps appearing after longer stays in the dark, although the amplitude distributions of both populations overlap. Lederhofer [18] and Lederhofer *et al.* [19] could show that these differences in size can be explained readily by the higher

percentage of bump overlapping of the more frequent but not larger light-evoked bumps in the respective experiments.

The “light bumps”, observed during (dim) steady illumination and the bumps observed within the first second following a bump-evoking flash are then a mixed group containing both light-evoked and spontaneous bumps.

We term bumps following a flash after a delay of more than 1 s “dark bumps” or “spontaneous bumps”, although strictly speaking this group contains also some delayed light-evoked bumps.

With increasing energy of the bump-evoking light flash the individual bumps overlap and fuse to the “macroscopic” receptor current (or receptor voltage) signal in which individual bumps are no longer discernible [20] (Fig. 1).

Bumps can be recorded as membrane voltage signals (voltage bumps) or, under voltage clamp conditions, as membrane current signals (current bumps). Current bumps allow more direct insight into the bump-generating mechanism. Size and shape of voltage bumps are secondarily modified due to voltage-sensitive conductances (*e.g.* regenerative components) and saturation phenomena. We have reported previously distributions of sizes and latencies of voltage bumps in dependence of light adaptation and extracellular calcium concentrations [17, 21]. In this paper we continue our bump studies dealing only with current bumps recorded from the ventral nerve photoreceptor cell of *Limulus* under voltage clamp conditions.

The aim of this study is to obtain more easily interpretable parameters characterizing bump properties of the *Limulus* photoreceptor in the dark-adapted state and at various degrees of weak light adaptation. We use conditioning pre-illumination while the photoreceptor cell is bathed in a saline of normal physiological ion concentration, or of lowered calcium concentration together with normal or raised magnesium concentration.

We have previously reported [22] magnesium ions to antagonize only part of the effects of lowering calcium (those on the dark conductance and on the extent of the light-induced conductance increase, but not those on the time course) on the receptor potential of the *Limulus* photoreceptor. We therefore proposed that the effect of calcium deficiency which is not antagonized by raised magnesium is to prolong the bump latencies following a

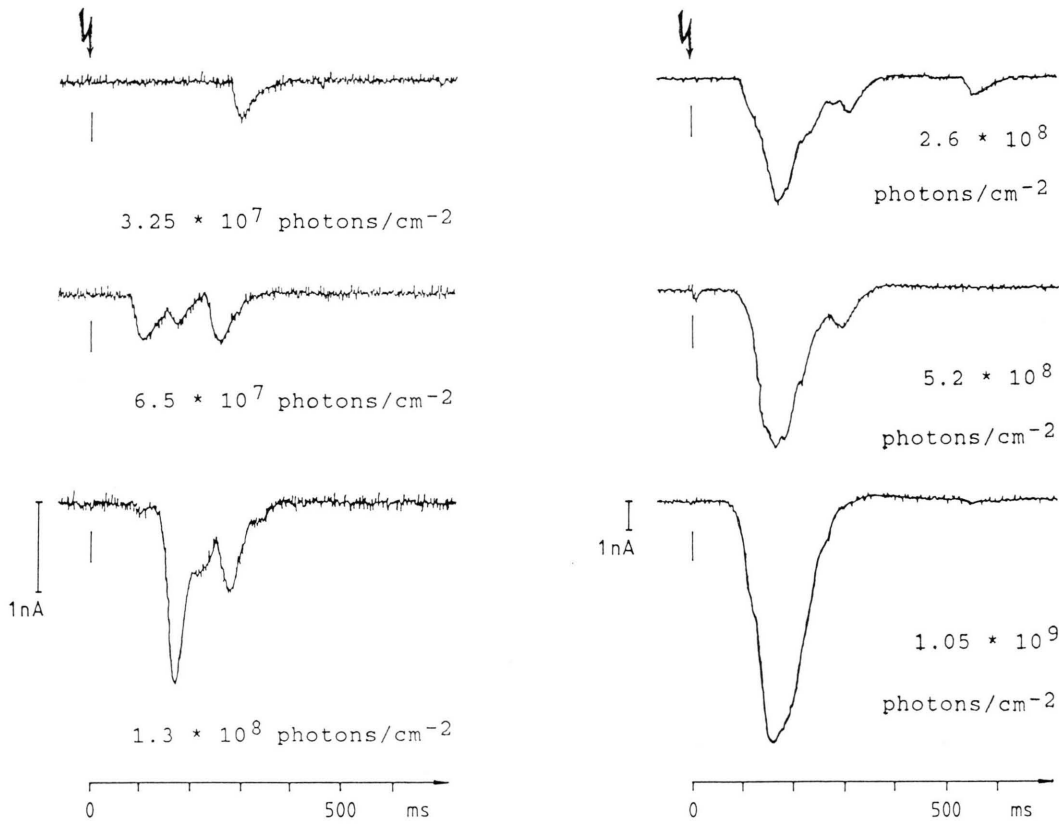


Fig. 1. Recordings of the receptor current signal of the *Limulus* ventral nerve photoreceptor in response to 50–1000 μ s light flashes of different energies. Individual bumps occur at low stimulus energy, they overlap and fuse at higher energy to form the smooth macroscopic receptor current signal. bt 130788, 15 °C.

flash. To further investigate the action of calcium and magnesium by direct bump observation we compared the effect of lowered external calcium concentration either together with normal magnesium concentration or with magnesium raised two-fold to 100 mmol/l on various bump parameters.

Some of the results have been previously reported in a shortened version [20, 23–25].

Model of bump generation

In previous publications we have investigated a number of bump parameters [17] and described a model for the mechanism of bump generation [23–25]. Starting from this model we want to discuss the phenomena investigated here:

The main characteristics of this model (Fig. 2) which has been developed in cooperation with J. Schnakenberg and W. Keiper are: Photoiso-

merization of one rhodopsin molecule in a microvillus initiates a sequence of reactions which causes after a variable delay (mostly between 10–500 ms, the latency) the activation of an enzyme (cascade) which finally leads to the activation of a source Q of internal transmitter T or messenger. This may be situated at the basis of the microvillus which is hit by the photon. The messenger source thereupon produces, activates or releases many messenger molecules which are formed from precursors. The time of increase in amount of active transmitter determines the rise time of the bump. The messenger T diffuses along the bases of the microvilli and is bound by the ion channels Ch which may be situated close to the bases of the microvilli. Following transmitter binding (presumably 4 or 5 transmitter molecules per channel [23, 26, 27], the ion channels are transiently opened. When the activity of the source Q dwindles, the amount of ac-

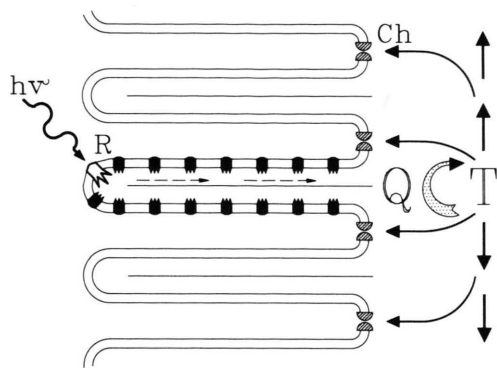


Fig. 2. Schematic diagram of proposed mechanism of bump generation. A light-activated rhodopsin molecule R in the microvillus starts the activation of an enzyme cascade which finally leads to the activation of a messenger source Q. The messenger (internal transmitter) T diffuses along the bases of the microvilli and is bound by the ion channels Ch which may be located close to the base of the microvilli. An ion channel opens when it has bound n (possibly 4 or 5) transmitter molecules. Thus a more or less circular "bump speck" of transiently open channels develops with a diameter of up to about $4\ \mu\text{m}$. The average bump speck of a light-adapted photoreceptor cell is smaller. The bump current amplitude is proportional to the number of simultaneously opened ion channels and should therefore be more or less proportional to the area of the bump speck (see text).

tive transmitter and consequently the number of simultaneously opened ion channels decreases too. The latency ends when the first channels open. The bump size is not correlated with the latency *i.e.* during the latency the amplification is negligible in the *Limulus* photoreceptor in contrast to the vertebrate photoreceptor.

Up to now the terminal excitatory messenger of the microvillar photoreceptor has not been identified. Cyclic GMP or calcium ions mediated *via* IP_3 are possible suspects [28, 29].

Messenger diffusion and binding spreads the growing area of the photosensory membrane occupied by a bump (the "bump speck") probably to a diameter of up to about $4\ \mu\text{m}$ in the dark-adapted visual cell [27, 30]. One bump may cause the transient opening of 1000–10,000 ion channels corresponding to an area containing about the same number of microvilli. Feng *et al.* [31] directly measured the size of bump specks in the retinula cell of the fly *Sarcophaga*. Large bump specks had diameters up to $1\ \mu\text{m}$ corresponding to the involvement of a few hundred microvilli. According

to our model the average diameters of the bump specks become smaller with increasing light adaptation. The bump amplitude is roughly proportional to the number of simultaneously opened ion channels and thus more or less proportional to the area of the bump specks. The bump speck is surrounded by a large "corona" region which contains channels having bound a smaller number of transmitter molecules than necessary for the opening [24, 27].

The processes leading from light-activation of rhodopsin to the activation of the messenger source Q are responsible for the latency. The large scatter of latencies indicates that only a few molecules are involved in the reactions which determine the duration of the latency. In our model the bump rise is determined by the transmitter diffusion over the growing bump speck and the rise and decay of the transmitter concentration.

The high amplification which results in the opening of up to thousands of ion channels during one bump leads to the assumption that a much larger number of transmitter molecules have to be formed, released or activated in the process of bump generation. This large amplification is brought about by enzymatic reactions. In vertebrate photoreceptor cells an enzyme cascade could be demonstrated which causes the degradation of up to 10^6 cGMP molecules per activated rhodopsin molecule [32, 33]. The high amplification is responsible for the high maximal sensitivity of the *Limulus* ventral photoreceptor, enabling the cell to detect single photons way above the noise level. The great variation in size of bumps evoked by photons of the same wave-length under identical experimental conditions indicates that reactions of only a few molecules seem to control the amplification which determines the bump size.

The *decline* of the bump is determined according to our model by the decrease of the transmitter concentration convoluted with the stochastics of the closing of the ion channels. Nagy [10] and Nagy and Stieve [9] found two different light-activated ion channels with mean open times of 1.5 ms (12 pS channel) and *ca.* 5.5 ms (30 pS channel). The bump decline has a half time of decay of *ca.* 20 ms in the dark-adapted and 12 ms in the light-adapted state [4, 34]. Thus the bump decay may be determined both by transmitter waning and by the stochastics of channel closing kinetics. We will use

this model as a plausible synaptic framework to discuss and interpret our experimental results.

Materials and Methods

Bumps were recorded as membrane current signals while the membrane voltage was clamped to the dark potential (−30 to −40 mV). Two intracellular electrodes in a ventral nerve photoreceptor cell of *Limulus* were used in a standard way [35]. The ventral nerve in an experimental chamber was continuously superfused with saline of 15 °C which could differ in ionic composition. The composition of the salines used is described in Table I.

Table I. Composition of salines (mmol/l).

[mmol/l]	KL 069–083		KL 086–090	
	PS	Low Ca	PS	Low Ca High Mg
Na ⁺	440	449	471	418
K ⁺	10	10	10	10
Ca ²⁺	10	0.25	10	0.25
Mg ²⁺	55	55	55	100
Cl [−]	515	505	606	623
SO ₄ ^{2−}	30	30	0	0
HEPES	10	10	10	10

Two types of light stimuli were used, both filtered through a broadband interference filter, lambda max 540 ± 40 nm (half width):

1. A bump-evoking xenon flash from a photo flash source (Metz 60CT-1/2), of a duration of 50 µs; repetition time 10 s. The light energy E_e ca. 1×10^8 photons cm^{−2}.
2. A conditioning, light-adapting flash, duration 10 ms, from a xenon lamp: Maximal energy E_c at the photoreceptor 10^{10} photons cm^{−2}; it could be attenuated by neutral density filters; the conditioning flash was applied 2 s prior to the bump-evoking flash.

In a period of 8 s following the bump-evoking flash the measured membrane current was digitized with a frequency of 1 kHz, stored on tape and later evaluated by a computer program. It recognized bumps with amplitudes larger than the 20–50 pA noise level which varied from cell to cell. Accuracy of measurements was 2.5–5 pA and 1 ms.

Evaluation

Bump parameters

In order to characterize bump size and shape we determined a number of bump parameters by means of a computer evaluation program (Fig. 3a):

- TLAT [ms], latency, the time from stimulus onset to the first measurable deflection of the current from the baseline above noise.
- A [nA], amplitude of bump maximum.
- TA [ms], time-to-peak: the time from stimulus onset to the maximum of the bump. TA can be determined for every recognized bump.

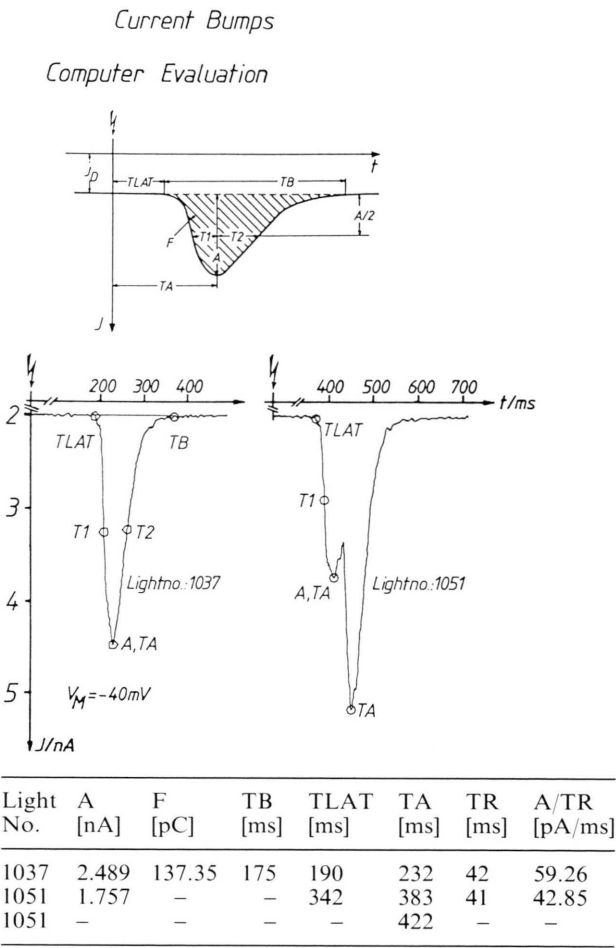


Fig. 3. (a) Bump parameters which were determined by computer. Two recordings from experiment KL098 show where the program fixes the values for the parameters.

TR [ms], rise time (TA–TLAT), the time from the detectable beginning of the bump to the bump maximum.

A/TR [nA/ms] the average steepness of bump rise.

TB [ms], bump-width: time from the end of the latency until the current has returned into the baseline noise.

F [pC = nA·ms], area: current-integral of the bump over TB.

Bumps were frequent during the first second after the bump-evoking flash and became rare in the following seconds. Three different types of bumps were distinguished and different parameters were determined of them:

– Apparently single bumps: all parameters were determined.

An unknown percentage of overlapping bumps were mistaken for single bumps since they were totally overlapping superpositions of more than one bump; here we have no means of certain recognition. In the distribution of apparently single bumps (see *e.g.* Fig. 5) the larger, and longer bumps contain a greater fraction of multiple bumps than the smaller, shorter bumps.

– Apparently overlapping bumps:

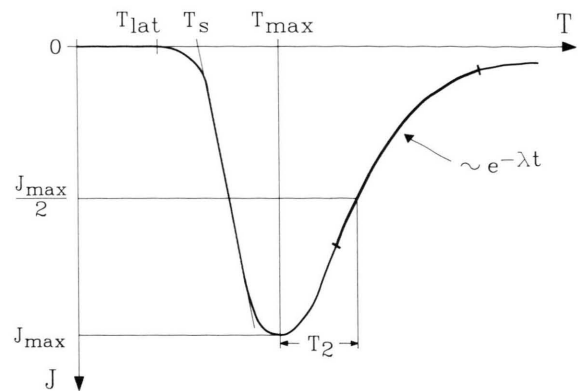
– – “Riders”, bumps riding on top of a preceding bump: only TA, the time-to-peak was determined. Their number is counted as NR.

– – “Horses”: bumps having a rider on top after the maximum: TLAT, TA and A were determined only.

Bump sum parameters

We calculated the normalized “bump sum” and measured their parameters (Fig. 3b) to characterize general average features of the bump responses. The bump responses to 50–150 individual flashes were linearly summed up for each sample time (every ms) following the bump-evoking flashes. The current values of the resulting sum curve were then scaled, divided by the number *N_s* of applied flashes. The normalized bump sum is an average response to the bump-evoking light flash and depends upon the number, sizes and predominantly upon the time of occurrence (characterized by latency or time-to-peak) and to a much lesser degree upon the widths of the bumps following a flash.

The bump sum has a characteristic shape (Fig. 3b): after a latency a smooth rise is followed



Bumpsum 1990

Fig. 3. (b) The parameters of the normalized bump sum, obtained by summation of 50 to 100 bump responses recorded under identical conditions. TLAT: latency; TMAX: time-to-peak; T2: half-time of decay and Λ : time constant of the exponential decay.

by an almost linear rising part, which amounts to more than 80% of the rising phase. Its decline after the maximum and a transition period can be approximated by an exponential. We measured the amplitude *A* of the maximum and the current-integral *F* (area). The latency of the bump sum can be determined only inaccurately due to rare bumps with short latencies. In addition we measured the time-to-peak and the half-time-of-decay and determined the rate constant Λ of the exponential decay.

The bump sum represents a convenient, but complex measure of the average number, average size and the latency distribution of the bumps evoked by dim flashes under various experimental conditions. It is mainly determined by the time-to-peak (TA) distribution of the underlying bumps. The time of the maximum should coincide with the maximum of the bump TA distribution. Only the latency of the bump sum depends on the number of summed responses. The argument is as follows:

The latency of the bump sum is that of the bump with the shortest latency which exceeds the noise. It should be the shorter, the larger the number of the summed responses is, since the probability for rare short latencies increases with the number of trials. The amplitude of the bump sum (Table III, A/N_s) is much smaller than the average bump amplitude, since the bump maxima are not in phase

Table II. Average bump parameters of first bumps (KL098) recorded in physiological saline; dark-adapted ($E_c/E_e = 0$) and weakly light-adapted ($E_c/E_e = 97$). A, amplitude; F, current-integral; TB, duration; TLAT, latency; TR, rise-time; A/TR slope of signal rise. Evaluation of the first 2 s of the responses to 250 flashes each; F and TB from all first and apparently single bumps. A, TLAT, TR and A/TR from all first bumps. See Fig. 4 for further experimental details.

KL098	Bump parameters					
	Means	$E_c/E_e = 0$	N	Means	$E_c/E_e = 97$	N
$\langle A \rangle$	1.75 ± 0.07	[nA]	221	0.69 ± 0.03	[nA]	206
$\langle F \rangle$	88 ± 7.2	[pC]	120	27 ± 1.7	[pC]	132
$\langle TB \rangle$	132 ± 4.1	[ms]	120	94 ± 2.3	[ms]	132
$\langle TLAT \rangle$	199 ± 11	[ms]	221	154 ± 15	[ms]	206
$\langle TR \rangle$	41 ± 1.1	[ms]	221	31 ± 0.9	[ms]	206
$\langle A/TR \rangle$	42 ± 1	[pA/ms]	221	23 ± 1	[pA/ms]	206

in the bump sum due to the fluctuating times-to-peak. The current-integral (area) of the bump sum divided by the number of recognized bumps which contribute to the bump sum F/N_b is larger than the average area of the individual involved bumps because not all bumps are recognized by our evaluation program (they may be hidden in the noise or disguised by total bump overlap). The area of the bump sum divided by the number of stimuli F/N_s is a direct measure; it represents the average area of the response to a single stimulus to which also those bumps contribute which are not individually recognized because they are hidden in the noise.

Procedure

The stimulus program is shown in Fig. 4. It was repeated 50 to 250 times. The light energy of the bump-evoking flash was adjusted so as to evoke bump responses in about 50% of the trials. However, in most experiments the sensitivity of the impaled cell increased during the experiment, so that on the average 2 to 3 (up to 5) bumps were evoked per flash (Table III, N_b/N_s). Two seconds prior to the bump-evoking flash a conditioning flash of variable energy could be administered to study the effect of pre-illumination on the bump responses evoked by the constant bump-evoking flash.

Most of the bumps occurred within the first second after the bump-evoking flash. During the following 7 seconds bumps were considerably less frequent (*ca.* 0.1/s compared to *ca.* 1–3/s during the

first second). Under the following two assumptions we estimate that less than 5% of the bumps found in the first second are spontaneous bumps: 1) The rate of the spontaneous bumps is constant during the 8 s cycle time. 2) The vast majority of the bumps in the 6th and 7th second are spontaneous bumps, whereas practically all the bumps occurring within the first second are due to the bump-evoking stimulus.

When different superfusates were tested the experiments started with a pre-period of about 15 to 25 min during which the nerve was superfused by physiological saline. A stimulus series where only the bump-evoking flash was applied was repeated 50–100 times. Then a conditioning flash of variable intensity was administered additionally in each stimulus cycle (E_c/E_e between 16 and 250), again 50–100 times. The perfusion of the chamber was then switched to a test saline (test period) and the stimulation continued by bump-evoking flashes only. (The perfusion of the chamber needed *ca.* 5 min to replace 95% of the bathing saline). The measurements started 15 min after the switch by two successive periods of 50–100 bump-evoking stimulations first without and then with the conditioning pre-illumination. During the exchange of the bathing saline the bump-evoking stimulus was administered every 10 s but the responses were evaluated not earlier than 15 min after the switch.

The responses to the bump-evoking stimuli were recorded, measured individually, and the distribution of parameters plotted.

The experiments lasted between 2 and 4 h.

Table III. Parameters determined from bump sums, *i.e.* summed bump responses. E_c : energy of bump-evoking flash. E_c/E_e : quotient of energies of conditioning to bump-evoking flash, Ns: number of stimuli, Nb: number of recognized bumps, A: amplitude, F: current-integral, TLAT: latency, TMAX: time-to-peak, T2: half-time of decay of the bump sum.

Experiment	E_c/E_e	$\left[\frac{E_c}{10^8 \text{ Ph}} \right]$ [cm ²]	Ns	Nb	Nb/Ns	A/Ns [nA]	F/Ns [pC]	F/Nb [pC]	TLAT [ms]	TMAX [ms]	T2 [ms]
KL065	0	0.45	51	101	2.0	0.29	51	25.8	130	260	125
	0.01		51	89	1.7	0.29	52	29.5	90	255	125
	0.12		51	102	2.0	0.63	120	60.0	75	225	100
	2.1		51	95	1.9	1.56	241	129.0	80	210	75
	35		51	93	1.8	0.82	114	62.5	40	150	80
	140		51	82	1.6	0.24	23	14.5	40	120	55
KL067	0	0.98	100	253	2.5	0.42	89	35.1	75	250	90
	0.06		100	310	3.1	0.90	166	53.5	75	230	90
	1		100	364	3.6	1.20	215	59.0	60	190	85
	16		100	364	3.6	1.10	152	41.8	50	180	60
	64		100	387	3.9	0.60	89	23.0	40	175	50
KL068	0	0.98	100	373	3.7	0.57	120	32.2	100	240	130
	0.06		100	565	5.7	0.90	169	30.0	75	220	90
	1		100	582	5.8	0.90	155	26.6	70	200	85
	16		100	595	6.0	1.12	152	25.5	55	160	70
	64		100	467	4.7	0.70	82	17.5	50	140	50
KL073	0	1.15	100	366	3.7	1.27	262	71.7	70	210	105
	0.3		50	182	3.6	1.52	336	92.2	80	230	120
	6.5		50	181	3.6	1.82	344	94.9	90	220	90
	26		50	137	2.7	1.42	272	99.4	80	230	90
KL083 (PS)	0	0.57	94	342	3.6	0.55	200	55.0	125	350	160
	35		100	349	3.5	0.70	154	44.2	100	270	140
	140		50	107	2.1	0.35	92	42.9	80	230	105
KL083 (Low Ca)	0	0.57	101	489	4.8	0.80	461	95.2	170	490	400
	35		100	482	4.8	0.83	384	79.7	150	470	230
	140		50	155	3.1	0.50	184	59.4	140	330	190
KL090 (PS)	0	0.48	50	112	2.2	0.77	45	20.0	180	400	100
	16		49	102	2.1	0.32	63	30.3	120	300	90
	256		49	59	1.2	0.10	27	22.5	100	280	100
KL090 (Low Ca, High Mg)	0	0.48	50	180	3.6	0.34	198	55.0	190	800	280
	16		50	214	4.3	0.54	261	114.0	90	600	200
	256		50	149	4.0	0.12	36	9.0	150	450	80
KL098	0	0.82	250	495	2.0	0.65	125	62.5	75	220	100
	97		250	401	1.6	0.40	61	38.1	50	150	75

Results

Dark-adapted photoreceptor, physiological saline

Individual bumps

If the dark-adapted photoreceptor cell of *Limulus* is stimulated by light flashes which are so weak that not every flash evokes a light response, one observes bump responses (Fig. 4, left column).

It can be seen that

1. the bumps follow the flash after considerable and greatly variable delay times (latencies) between 50 and 500 ms,

2. the size of the bumps also varies greatly although the bumps are all evoked by identical stimuli, *i.e.* photons of the same wave-length.

3. the number of recognized bumps following the flash varies, it can be 0, 1, 2 ..., again although the stimuli are identical (not shown in Fig. 4, left column).

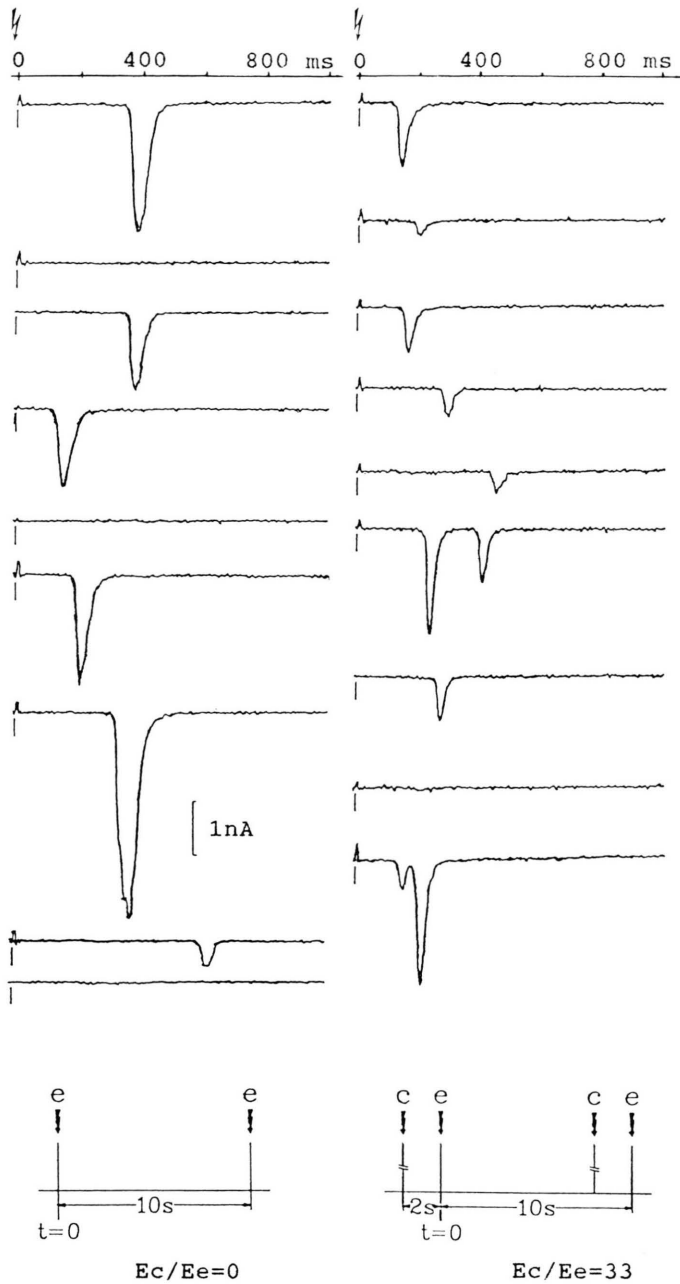


Fig. 4. Current bumps measured under voltage clamp. Superfusate: Physiological saline. Left column: dark-adapted photoreceptor ($E_c/E_e = 0$); right column: photoreceptor weakly light-adapted by a conditioning pre-illumination two seconds prior to the bump-evoking flash ($E_c/E_e = 33$). Bump-evoking flash: $E_e = 6 \times 10^7$ photons/cm², duration 50 μ s, repetition time 10 s; conditioning, light-adapting flash: $E_c = 2 \times 10^9$ photons/cm²; both flashes 540 nm, membrane potential clamped to -40 mV. Bottom: stimulus regime. KL096, 15 °C.

Fig. 5 shows the frequency distributions (histograms) of some bump parameters, Table II the average values of the same experiment. The bump amplitude is variable. It can be as large as 5 nA. The rare, very large bumps (5 nA) may be – at least in part – the result of complete superposition of 2 or more bumps. We do not know the smallest

bump size. We can only detect bumps if their amplitudes are larger than the 20–50 pA noise level of our registrations. There may be many smaller bumps hidden in the noise.

We can estimate a lower limit for the smallest bump: If we assume that the smallest bump is due to the opening of a single ion channel its amplitude

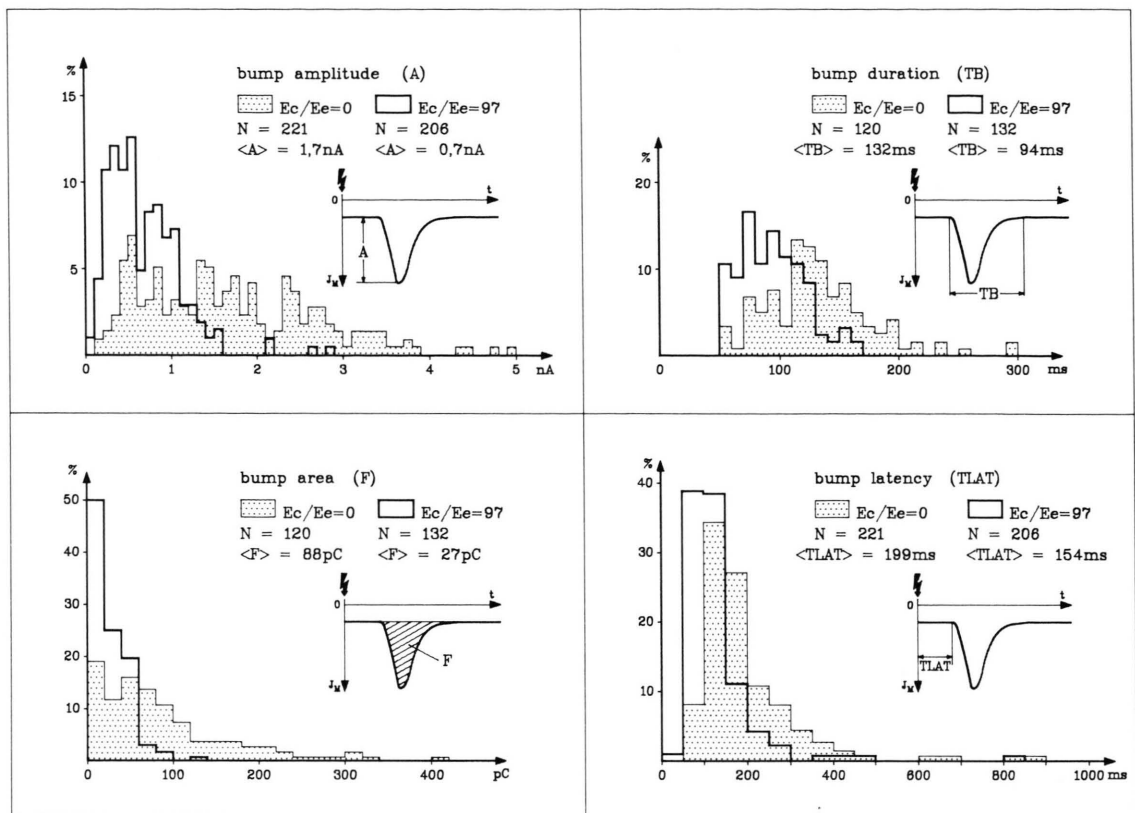


Fig. 5. Frequency distributions of bump amplitudes (A), bump current-integrals (F), bump durations (TB), and bump latencies ($TLAT$) of a *Limulus* ventral nerve photoreceptor cell in dark-adapted ($E_c/E_c = 0$) and weakly light-adapted ($E_c/E_c = 97$) conditions. Latencies and amplitudes are plotted of all first bumps following the bump-evoking flash; current-integrals and bump durations of all first and single bumps. N is the number of the bumps accounted for, $\langle A \rangle$, $\langle F \rangle$, $\langle TB \rangle$, $\langle TLAT \rangle$ are the arithmetical averages of bump parameters. KL098, see Fig. 4 for further experimental details.

would be between 0.5 and 2 pA near dark potential (see above, [5–7, 9, 10]). Under our experimental conditions this would mean that more than 10 ion channels must open simultaneously to exceed the noise level of 20–50 pA. All smaller bumps would remain undetected.

Most bump parameters (Fig. 5) have bell-shaped, more or less asymmetric frequency distributions except for the histogram of the bump current-integrals F (areas) which often displays a monotonously falling distribution. However, a substantial percentage of cells show asymmetric, more or less bell-shaped area distributions (for instance [20], Fig. 3 and 4). Goldring [36] and Grzywacz and Hillman [37] found exponentially falling distributions.

The bump duration TB in the dark-adapted cell is between 50 and 300 ms, on the average about 130 ms; it is substantially shorter than the latency, on the average by a factor of 0.6. The bump rise TR lasts on the average about 40 ms, it is about one third of the bump duration.

The bump latency $TLAT$ varies between 20 and 900 ms, on the average about 200 ms; its frequency distribution is the most asymmetric of all bump parameters.

The variations of size and latency of the light-evoked bumps under identical stimulus conditions and at identical level of adaptation are not correlated with each other [17, 38, 39].

Furthermore, Keiper [4] and Keiper, Schnakenberg and Stieve [25] have shown that four “prima-

ry" bump parameters (latency TLAT, rise time TR, maximal slope m of rise and time constant λ of bump decline) are not correlated with one another, whereas bump amplitude and current-integral are "secondary" parameters, depending mainly on slope and duration of the bump rise.

Bump sum

The normalized bump sum gives information about the average response of the photoreceptor cell to weak stimuli. In Table III characteristic data of a number of bump sums are listed. Fig. 6 shows an example of a bump sum. From its area 30.9 pC one calculates for the dark-adapted photoreceptor response an average response area to a flash $F/N_s = 125$ pC and an average bump area F/N_b of 62.5 pC (Table III). The value of the average bump area is smaller than the 88 pC determined for individual bumps of Fig. 5, because in the latter case only single bumps are surveyed which is a biased selection towards larger bumps. The value A/N_s is smaller than the average bump amplitude because of the large scatter in bump latencies.

Fig. 6 demonstrates that the time course of the bump sum is primarily determined by the time-to-peak TA distribution of the underlying bumps and not so much by the bump width TB since TMAX (and its variance) is large compared to TB. The latency of the bump sum is that of the bump with the shortest latency in the sample (if the size of the bump contributes significantly to the bump

sum). (In Fig. 6 the latency distribution is plotted only of the first bumps!)

The time parameters TLAT, TMAX, T2 of the bump sum of the dark-adapted cell vary greatly from cell to cell (Table III). However, the variation becomes small (less than 5%) when the parameters are normalized with respect to TMAX (TLAT/TMAX, T2/TMAX). Since the time course of the bump sum is primarily determined by the TMAX distribution, this indicates that the TMAX and the TLAT distribution varies from cell to cell by a scaling factor. Possibly small differences in temperature from experiment to experiment may contribute to these differences.

Light adaptation and facilitation

Individual bumps

The conditioning illumination 2 s prior to the bump-evoking flash caused two opposite types of changes in the bump response which follows the bump-evoking flash. – If the energy of the conditioning flash is strong enough ($E_c/E_e > ca. 32$) it causes *desensitization* (light adaptation). The bumps evoked by the bump-evoking flash are smaller and shorter than without the conditioning pre-illumination (Fig. 4, 5 and Table II, III). Bump size, *i.e.* amplitude A or current-integral F , distributions are shifted to smaller values and all time parameters are shortened by about the same factor but less than A and F . The bump latency is shortened too. Since the bumps become smaller and shorter by light adaptation, the bump area is

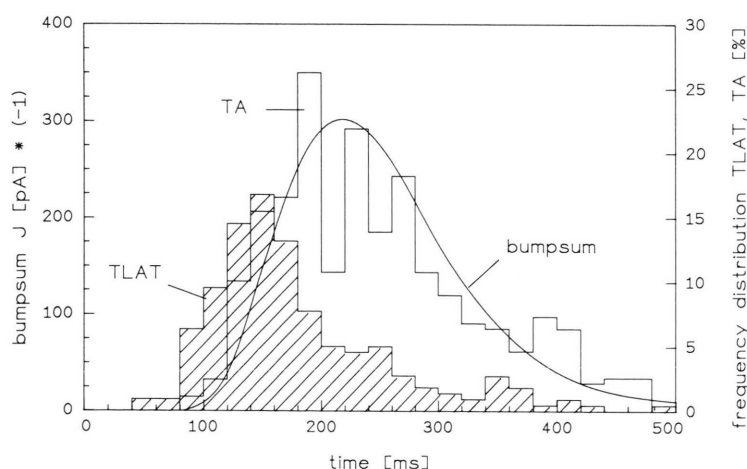


Fig. 6. Normalized bump sum and the corresponding frequency distributions of bump latencies (TLAT) and bump time-to-peak (TA) of the same experiment as Fig. 5. TLAT of all first bumps, TA of all recognized bumps. The responses to 250 bump-evoking flashes were summed. KL098, 15 °C.

more diminished than the bump amplitude. These changes are all gradual, the more pronounced the stronger the conditioning pre-illumination. The number of bumps per stimulus $(N + NR)/Ns$ identified in the first second of the cycle may be diminished or raised due to light adaptation (Table III), on the average it is diminished (Table IV).

– Very weak conditioning flashes ($E_c/E_e < ca. 16$), however, cause *facilitation*, an opposite effect: the bumps increase in size and number *i.e.* the number of bumps which are evoked by the constant bump-evoking stimulus is increased and their average size is enlarged (Fig. 7, 8, Table III).

Table III shows the evaluation of 7 experiments which demonstrate that the degree of facilitation and the ratio between the increase in bump size and in bump number differs from cell to cell. Experiment KL065 shows facilitation (an increase of F/Ns) with no increase in the number of bumps evoked per stimulus (Nb/Ns), whereas in KL068 the number of bumps is almost doubled; KL067 is an intermediate case. The cause for this variation may be differences in the efficiency of the bump-evoking stimulus.

In most cells the number of recognized bumps evoked per flash, (Nb/Ns , Table III), is increased due to facilitation and somewhat diminished after stronger illumination due to light adaptation. This decrease may be at least partially due to the diminution in bump size which increases the fraction of bumps below the noise level of recognition.

Facilitation is not restricted to light-evoked bumps. The bumps recorded in the 7th and 8th second of the cycle show the same tendency as those in the first second, *i.e.* bump enlargement and increased rate of spontaneous bumps (Table V). The bump rate seems to reach its maximum for dark bumps at higher energies of the conditioning pre-illumination than for the bumps observed in the first second of the cycle. Facilitation of the dark bumps is, however, in our experiments not statistically significant due to the small number of bumps found in the late phase of the cycle.

A corresponding observation was reported by us earlier [17]: A weakly light-adapting pre-illumination diminished the amplitudes and increased the rate both of light-evoked and of spontaneous bumps.

Fig. 7 shows that facilitation ($E_c/E_e = 1$) affects most bump parameters, *i.e.* amplitude A , bump area F , and bump duration TB are increased almost by the same degree due to facilitating pre-illumination. Stronger conditioning pre-illumination ($E_c/E_e = 64$) causes the opposite direction of changes, *i.e.* desensitization (light adaptation). The latency, however, behaves conspicuously differently from all other bump parameters. With increasing intensity of the conditioning flash the latency is shortened monotonously, showing no indication of two opposite effects for weak, facilitating and stronger, desensitizing pre-illumination.

This is demonstrated even more clearly in Fig. 8.

Table IV. Bump parameters (average values) of photoreceptors superfused by a) physiological saline, b) saline with calcium concentration lowered to 250 $\mu\text{mol/l}$, normal magnesium (Low Ca) and c) saline with calcium concentration lowered to 250 $\mu\text{mol/l}$ and magnesium concentration raised to 100 mmol/l . DA: dark-adapted photoreceptors ($E_c/E_e = 0$), LA: light-adapted photoreceptors ($E_c/E_e = 26, 64, 97, 140, 256$, see Table III); averaged values from 50 to 150 light numbers per experiment: A : amplitudes, F : current-integrals, TB : durations, $TLAT$: latency, TR : time of rise, A/TR : slope of signal rise, $(N + NR)/Ns$: number of recognized bumps per stimulus. 11 experiments (KL069–090), 15 °C.

KL069 – KL090		Phys. Saline Ca ⁺⁺ 10 mmol/l Mg ⁺⁺ 55 mmol/l Number of Exp.: 11		Low Ca Ca ⁺⁺ 250 $\mu\text{mol/l}$ Mg ⁺⁺ 55 mmol/l Number of Exp.: 6		Low Ca, High Mg Ca ⁺⁺ 250 $\mu\text{mol/l}$ Mg ⁺⁺ 100 mmol/l Number of Exp.: 5	
		DA	LA	DA	LA	DA	LA
$\langle A \rangle$	[nA]	0.93 \pm 0.13	0.78 \pm 0.10	1.66 \pm 0.23	0.79 \pm 0.17	1.14 \pm 0.17	0.79 \pm 0.05
$\langle F \rangle$	[pC]	46 \pm 8	32 \pm 6	111 \pm 18	40 \pm 18	95 \pm 12	38 \pm 6
$\langle TB \rangle$	[ms]	103 \pm 10	84 \pm 6	149 \pm 19	100 \pm 16	144 \pm 7	87 \pm 6
$\langle TLAT \rangle$	[ms]	311 \pm 26	249 \pm 25	432 \pm 40	330 \pm 31	647 \pm 56	417 \pm 87
$\langle TR \rangle$	[ms]	31 \pm 1.6	27 \pm 0.5	39 \pm 2.9	28 \pm 0.8	33 \pm 2.1	26 \pm 1.8
$\langle A/TR \rangle$	[pA/ms]	34 \pm 5.0	36 \pm 6.0	41 \pm 5.8	23 \pm 1.7	48 \pm 7.0	39 \pm 3.2
$\langle (N + NR)/Ns \rangle$		1.9 \pm 0.17	1.5 \pm 0.02	2.7 \pm 0.02	2.2 \pm 0.04	1.7 \pm 0.03	1.8 \pm 0.04

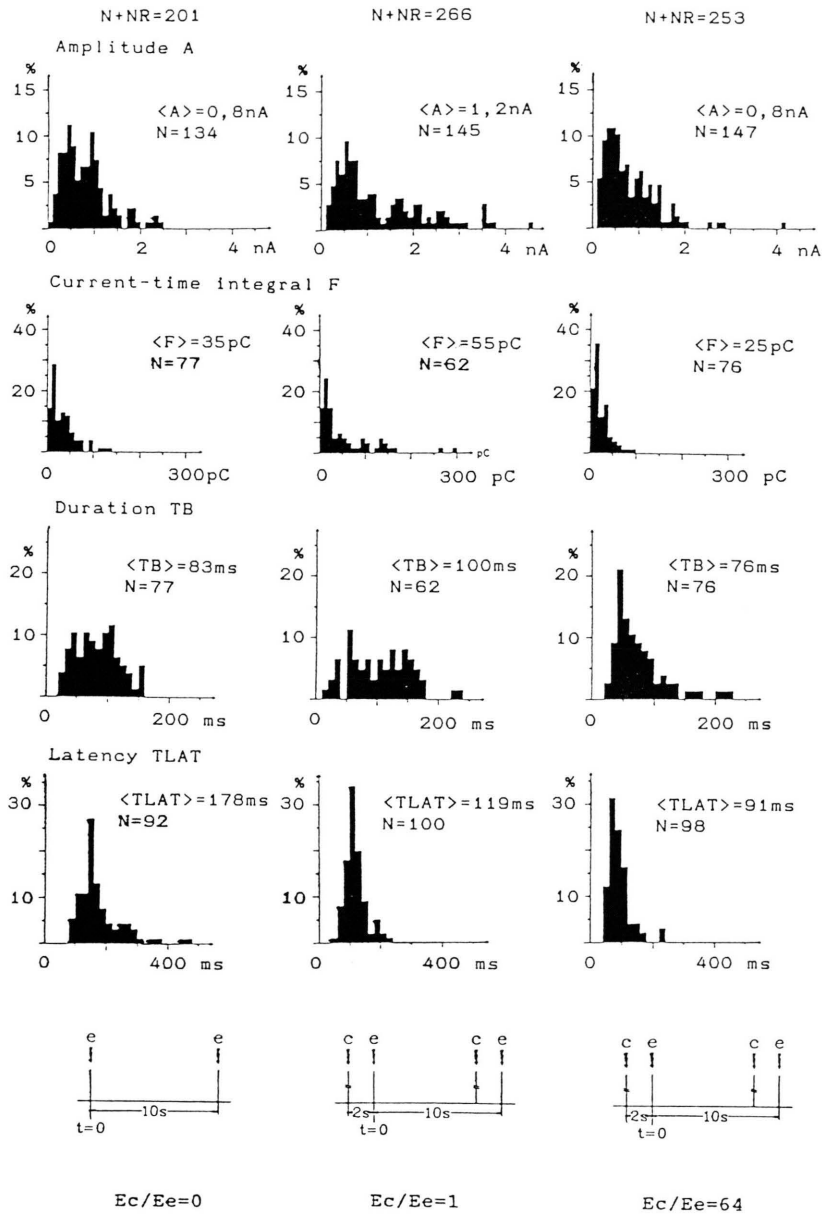


Fig. 7. Frequency distributions of bump parameters (amplitude A, current-integral F, duration TB, and latency TLAT) of *Limulus* ventral photoreceptors in three different states of adaptation. First column: dark-adapted ($E_c/E_e = 0$); second column: very weakly light-adapted ($E_c/E_e = 1$); third column: weakly light-adapted ($E_c/E_e = 64$). $E_e = 0.98 \times 10^8$ photons/cm². Distributions of amplitudes for all single and first bumps, current-integrals and durations for all single bumps, latencies for all first bumps, KL067, 15 °C.

The average parameters of the bumps recorded during the first second after the bump-evoking flash are plotted *versus* the relative energy of the conditioning pre-illumination. With increasing conditioning energy bump size F, amplitude A, and width TB are enlarged due to facilitation and diminished due to stronger conditioning illumina-

tion. The latency is the only parameter which changes (decreases) monotonously.

Hanani and Hillmann [40] found for barnacle photoreceptors under conditions of reduced sensitivity a similar dependence of the amplitude of the macroscopic receptor potential on the intensity of the conditioning pre-illumination. In contrast to

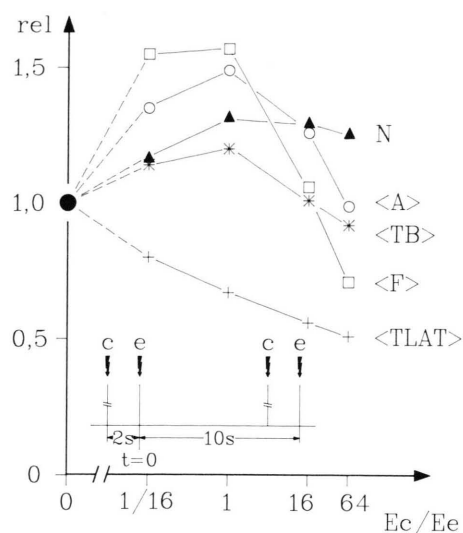


Fig. 8. Average bump parameters dependent on energy of pre-illumination demonstrating facilitation and desensitization. Ordinate: average value of bump parameter normalized with respect to the average value recorded in the dark-adapted state ($E_c/E_e = 0$). Reference values: bump frequency $\langle N + NR \rangle = 201$, bump amplitudes $\langle A \rangle = 0.83 \pm 0.045$ nA, bump durations $\langle TB \rangle = 83 \pm 4.0$ ms, bump current-integrals $\langle F \rangle = 35 \pm 3.3$ pC, bump latency $\langle TLAT \rangle = 178 \pm 7.5$ ms. Abscissa: quotient of conditioning to bump-evoking flash energy, $E_c = 0.98 \times 10^8$ photons/cm²; inset: stimulus regime. N: number of recognized bumps. KL067, same experiment as Fig. 7.

our results with the *Limulus* photoreceptor the facilitation of the barnacle photoreceptor was significantly augmented by reduction of the extracellular calcium concentration to 0.5 mmol/l.

Table V. Average bump parameters at different states of adaptation ($E_c/E_e = 0, 1/16, 1, 16, 64$). Comparison between first and seventh and eighth second of stimulus cycli. A: amplitude, F: current-integral, TB: duration, $(N + NR)/Ns$: number of recognized bumps per stimulus; 100 stimuli at each state of adaptation. KL067, 15°C.

	E_c/E_e				
	0	1/16	1	16	64
0–1 $\langle A \rangle$	0.83	1.13	1.25	1.05	0.82
6–8 [nA]	0.50	0.78	0.86	0.75	0.61
0–1 $\langle F \rangle$	35	55	55	37	25
6–8 [pC]	19	35	34	26	18
0–1 $\langle TB \rangle$	83	95	100	84	76
6–8 [ms]	69	92	86	79	57
0–1 $\langle \frac{(N+NR)}{Ns} \rangle$	2.0	2.4	2.7	2.6	2.5
6–8	0.11	0.21	0.22	0.37	0.45

Bump sum

Fig. 9 (see also Table III) shows five normalized bump sums of a photoreceptor cell a) in the dark-adapted state ($E_c/E_e = 0$), (b–e) with conditioning illumination of increasing energy ($E_c/E_e = 1/16$ to 64). The normalized size of the bump sum is *enlarged* due to the conditioning pre-illumination up to $E_c/E_e = 16$, the latency of the bump sum, *i.e.* the latency of the first occurring bump, is shortened and the whole time course of the bump sum is accelerated, *e.g.* the time-to-peak is shortened. Higher energy of the conditioning pre-illumination ($E_c/E_e = 64$) causes a *diminution* of the size

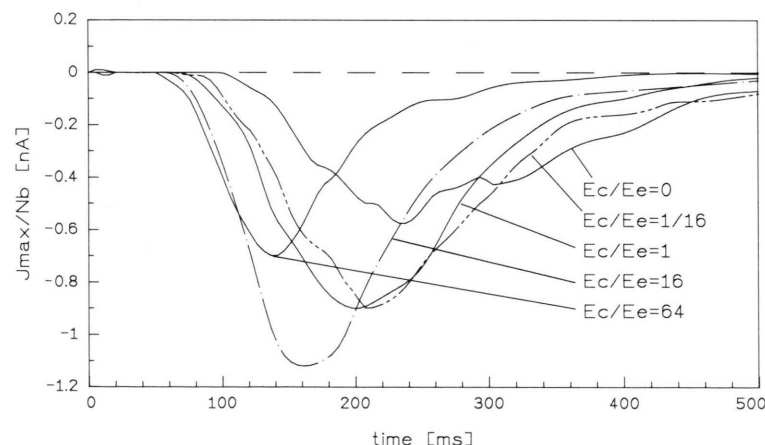


Fig. 9. Summed bump responses (normalized bump sums) to 100 very dim flashes at five different conditioned states due to pre-illumination by a conditioning flash of varied energy: E_c energy of conditioning flash, E_e energy of bump-evoking flash, $E_e = 0.98 \times 10^8$ photons/cm². KL068, 15°C.

and a further shortening of the latency and of the whole time course of the bump sum.

The time course of the bump sum is mainly determined by the latency (or time-to-peak) distribution of the individual bumps. Consequently the shortening of TLAT and TMAX of the bump sum in Fig. 9 and Table III indicates that both facilitation and desensitization shorten the bump latency monotonously. However, amplitude A and area F of the bump sum both pass through a maximum.

Lowered external calcium concentration (unchanged magnesium concentration)

In six experiments (Exp. KL069–083) bumps were recorded while the photoreceptor was superfused first with physiological saline and afterwards in the test period with a saline in which the calcium concentration was lowered to 250 $\mu\text{mol/l}$, all the other ion concentrations being unchanged (saline 2, Table I). Fig. 10 shows examples of recorded bump responses, Table IV average values of bump parameters of six experiments.

On the average the bumps of the *dark-adapted* cell are larger and longer in low calcium saline and the bump latencies longer. The frequency distributions of the bump parameters are broadened and shifted to larger values. The bump frequency is raised.

In closer detail:

Lowering the external calcium concentration from 10 mmol/l to 250 $\mu\text{mol/l}$ causes the following changes in the bumps of the dark-adapted photoreceptor (Table IV): The average size of the current bumps is greatly enlarged: the bump amplitude A to 180%, the bump area F even more (to 240%) since the average bump width TB is enlarged to 145%, the bump rise TR to 125%. The changes in these time parameters may be a consequence mainly of the enlargement of the bumps. The average slope of the bump rise A/TR is only slightly steepened to 120%. The average bump latency is prolonged to 140%. The number of bumps per stimulus (N + NR)/Ns identified in the first second of the cycle is raised to 140%.

These results are in some contrast to the behaviour of the voltage bumps upon lowering the external calcium to 250 $\mu\text{mol/l}$ [17]. Only the latency distribution was strongly affected, substantially shifted to longer latencies, whereas the average

amplitude and duration of the voltage bumps were only slightly enlarged. The frequency of spontaneous voltage bumps was slightly, not significantly raised. However, raising the external calcium concentration from 10 to 40 mmol/l caused an increase in generation of light-evoked and spontaneous voltage bumps [21].

The *bump sum* of the dark-adapted cell (Fig. 11) is greatly enlarged and broadened after lowering of the external calcium; enlarged due to an increase in number and size of the light-evoked bumps (Table III) and broadened due to the prolongation of the latencies of the underlying bumps. The area of the bump sum is therefore more than doubled (230%). The increase in number of bumps seems to be specific for light-evoked bumps: In experiment KL083 the frequency of the spontaneous bumps, observed in the 7th and 8th second of the cycle is about 0.06 bumps/s before and after the external calcium concentration is lowered.

Weak *light adaptation* does not significantly depend upon the external Ca^{2+} concentration, similarly as previously described for voltage bumps [17]. A conditioning flash ($E_c/E_e = 140$), 2 s prior to the bump-evoking flash, causes diminution of bump size and shortening of the time parameters of the bumps and of bump latency as described for physiological saline. The bump parameters are reduced in size by light adaptation to almost the same values as in physiological saline.

Figure 11 (see also Table III) shows the *bump sums* of such an experiment, dark-adapted and after conditioning pre-illumination of two different energies which both result in light adaptation (desensitization). It demonstrates that lowered external calcium concentration makes the bump sum larger and broader. Weak conditioning flashes ($E_c/E_e = 35$) may slightly increase the bump sum amplitude, they accelerate its time course significantly and thus narrow the bump sum. Stronger pre-illumination ($E_c/E_e = 140$) reduces the size and further shortens the bump sum. When the external Ca^{2+} concentration is lowered, pre-illumination has generally the same effect as in physiological Ca^{2+} concentration. Facilitation due to weak pre-illumination ($E_c/E_e < 16$) – indicated by an increase in F/Ns – was observed only in one of three experiments. Stronger pre-illumination causes light adaptation (desensitization). The changes in the bump sum due to pre-illumination are dominated by the

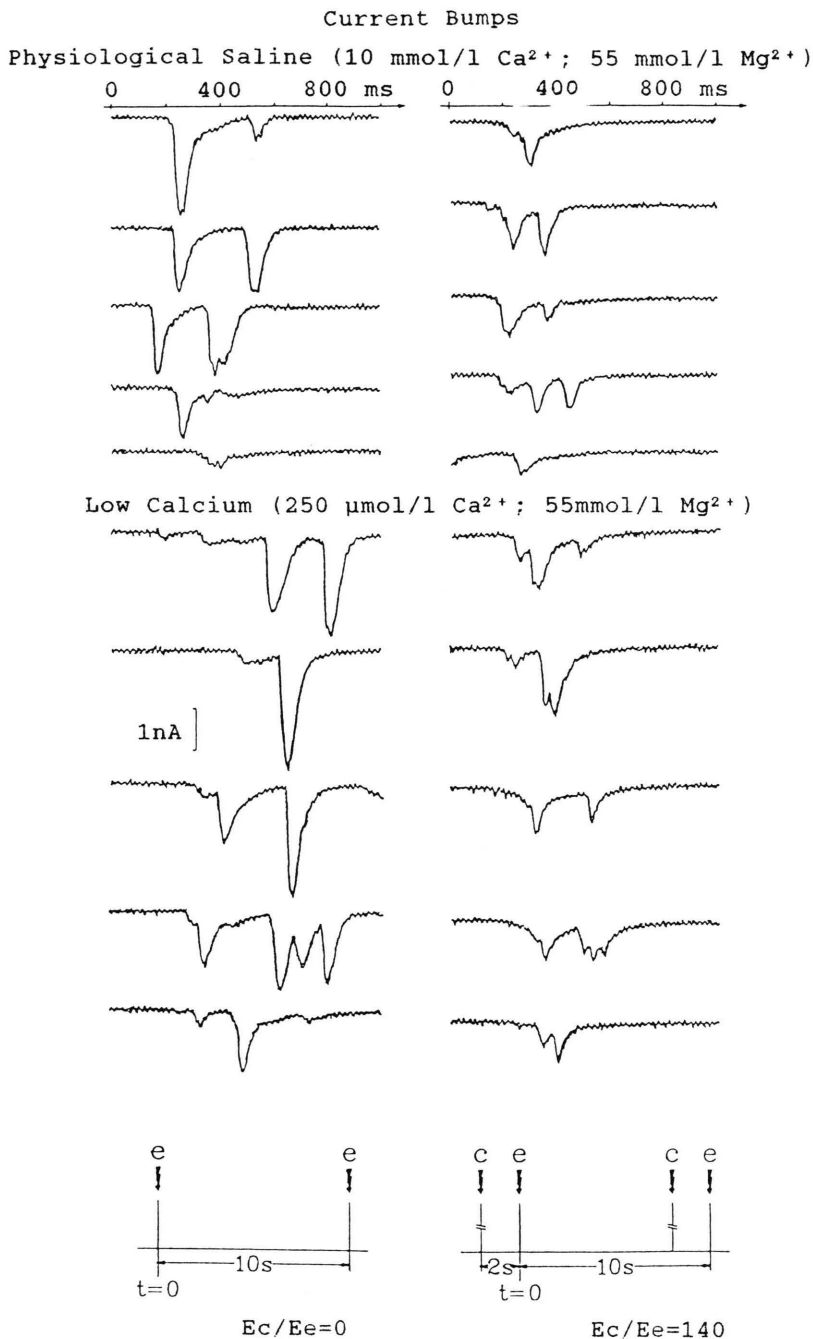


Fig. 10. Current bumps under voltage clamp conditions. Left column: dark-adapted, $E_c/E_e = 0$; right column: weakly light-adapted by a conditioning flash 2 s prior to the bump-evoking flash, $E_c/E_e = 140$, $E_e = 0.57 \times 10^8$ photons/cm²; upper half: photoreceptor was superfused by physiological saline containing 10 mmol/l Ca^{2+} , 55 mmol/l Mg^{2+} ; lower half: recorded while the photoreceptor was superfused with a saline of lowered Ca^{2+} (250 $\mu\text{mol/l}$) and normal Mg^{2+} (55 mmol/l). Otherwise same procedure as in Fig. 4. KL083.

pronounced shortening of the latencies of the underlying bumps, but changes in bump size and bump number are also observable (Table III and IV).

In Fig. 11 (see also Table III) the bump sum of the light-adapted photoreceptor ($E_c/E_e = 140$) in

low external calcium appears quite similar in size and shape as the bump sum of the dark-adapted photoreceptor ($E_c/E_e = 0$) in normal calcium saline. This suggests that the changes in the distribution of bump parameters of the dark-adapted

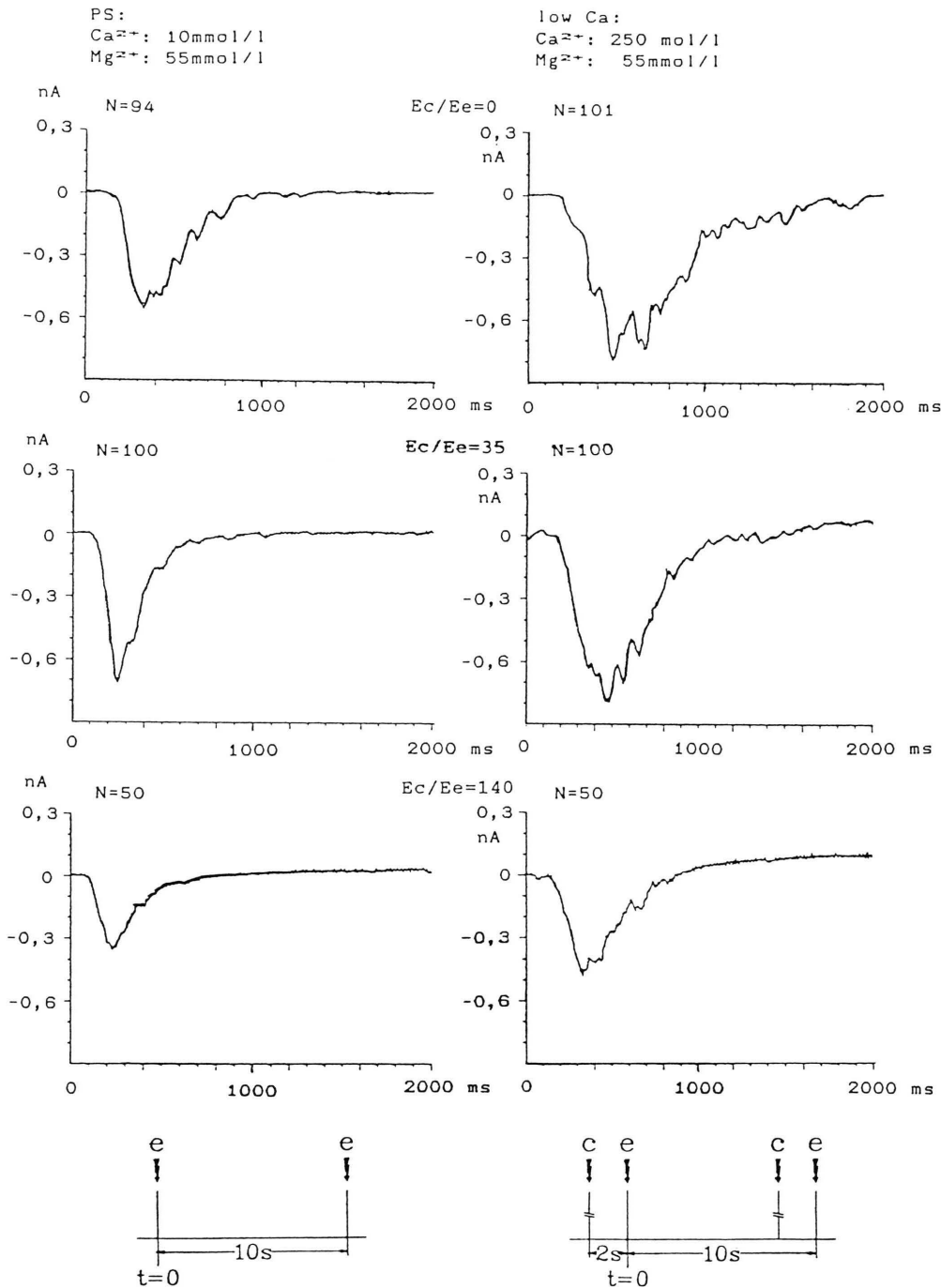


Fig. 11. Normalized bump sums. Summed bump responses to many very dim flashes in three different states of adaptation; left column: photoreceptor is superfused by physiological saline, right column: 40 min later the same photoreceptor superfused by a saline with 250 $\mu\text{mol/l}$ Ca^{2+} , normal Mg^{2+} ; N: number of summed bumpy responses. KL083, further details as in Fig. 6 and 9.

photoreceptor caused by calcium deficiency are based on an extra increase in dark adaptation.

Calcium concentration lowered to 250 $\mu\text{mol/l}$ and magnesium concentration raised to 100 mmol/l

In 5 experiments (KL086–090) the influence of lowering the external calcium and simultaneously

raising the external magnesium concentration on bumps of the dark-adapted photoreceptor or on the effect of conditioning illumination was tested. Compared to the experiments in which solely calcium was lowered while the magnesium concentration was kept normal (55 mmol/l) there were some conspicuous differences (Fig. 12, 13, and 14, Tables III and IV).

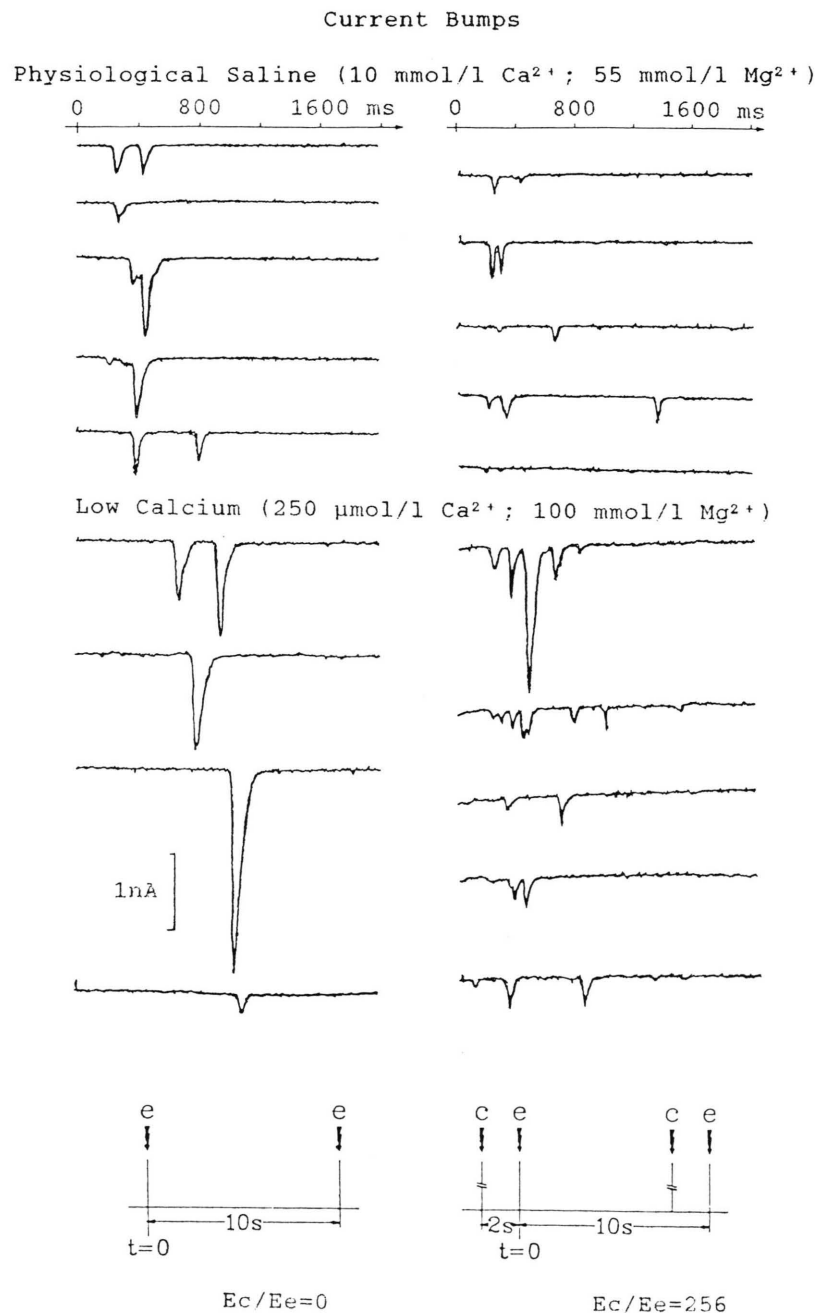


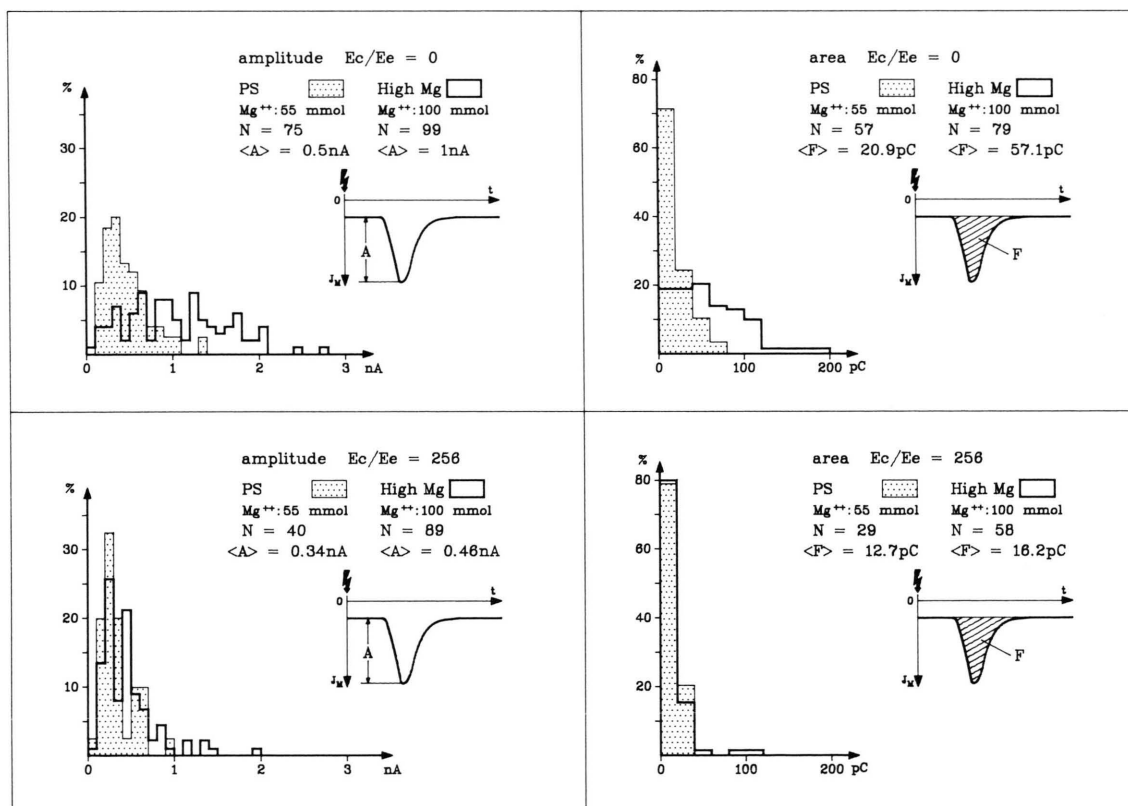
Fig. 12. Current bumps under voltage clamp conditions. Left column: dark-adapted ($E_c/E_e = 0$); right column: (weakly) light-adapted by a conditioning flash ($E_c/E_e = 256$); upper half: photoreceptor was superfused by physiological saline containing 10 mmol/l Ca^{2+} , 55 mmol/l Mg^{2+} ; lower half was recorded while the photoreceptor was superfused with a saline of lowered calcium concentration (250 $\mu\text{mol/l}$) and the magnesium concentration raised to 100 mmol/l . KL090, further details as in Fig. 4.

On lowering calcium and simultaneously raising the magnesium concentration in the bath saline of the *dark-adapted* photoreceptor (Table IV) the distributions of all parameters except for TLAT were changed not much differently than in lowered calcium alone. The bump size is enlarged somewhat less than when magnesium is not raised (bump amplitude A to 125%, bump area F to 210%); the average steepness A/TR of the bump rise is enhanced somewhat more (to 140%). The average time parameters of the bump (TB, TR) are not significantly different from those when only the calcium concentration is lowered. The latency, however, is much more prolonged (to 210% compared to 140%) than when calcium alone is lowered. The number of bumps identified in the first second of the cycle is sometimes increased, sometimes lowered. On the average it is not changed significantly.

The *bump sum* of the dark-adapted cell (Fig. 14, Table III) is greatly enlarged and broadened, on

the average a little less than when Ca^{2+} was lowered alone. Again the changes in the bump sum are due to an increase rather in the area than in the amplitude of the underlying bumps and in the broadening of the frequency distribution of the bump latencies.

Light adaptation is not much influenced by the external magnesium concentration: The conditioning pre-illumination ($E_c/E_e > 30$) of the photoreceptor bathed in saline of lowered calcium concentration causes the diminution of all bump parameters – except for the latency TLAT – to about the same absolute values as in physiological Ca^{2+} concentration, no matter whether the Mg^{2+} concentration is normal or doubled. The bump latency, however, is even less shortened when the magnesium concentration is raised. Very weak pre-illumination ($E_c/E_e < 16$) causes *facilitation* again both by enlargement of size and number of bumps following the bump-evoking flash. Here too, the



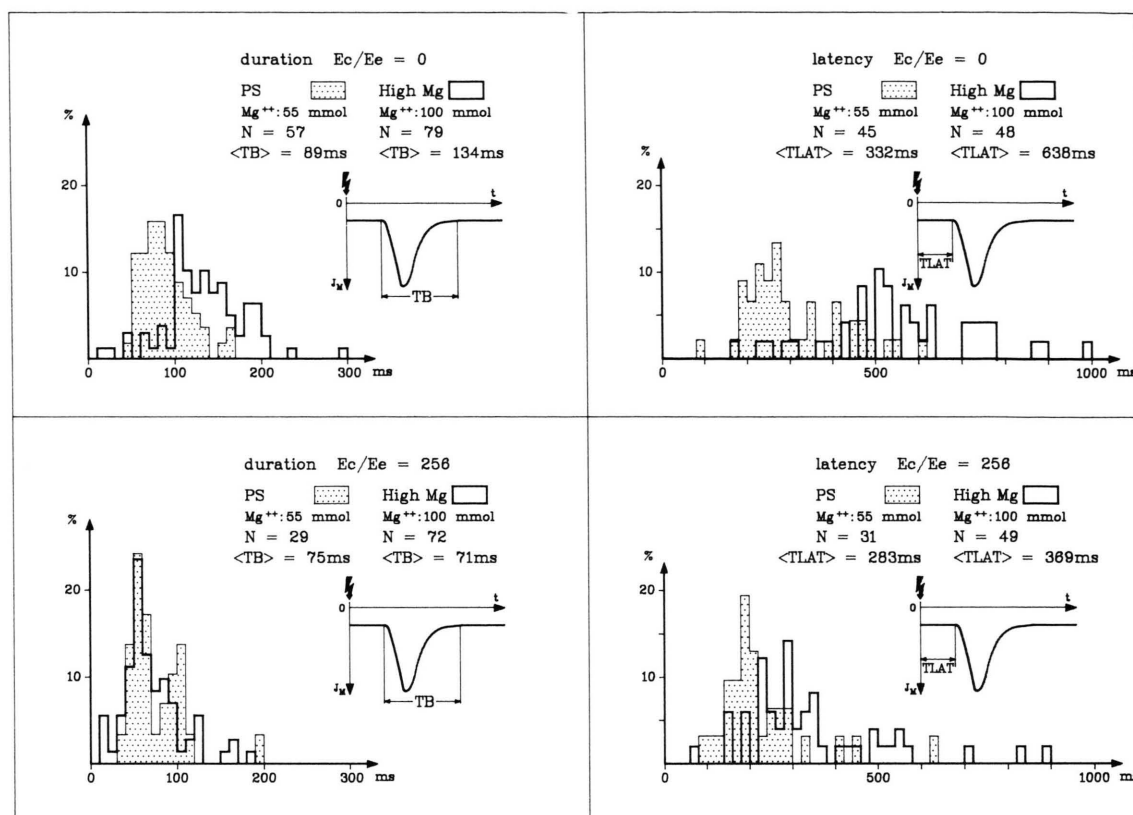


Fig. 13. Frequency distributions of bump parameters of a *Limulus* ventral photoreceptor superfused by physiological saline and by saline with lowered calcium and raised magnesium concentration (for concentrations see Fig. 12) in two states of adaptation ($E_c/E_e = 0$ resp. 256). KL090, further details as in Fig. 5.

latency is already shortened due to facilitating preillumination.

The *bump sum* shows the corresponding behaviour (Fig. 14 and Table III). Facilitation is seen based on an increase in number and size of the bumps evoked by the weak conditioning flash ($E_c/E_e \leq 16$, three experiments). Stronger conditioning energy causes reduction in size of the bump sum and of the underlying bumps (F/N_b) and drastic shortening of all time parameters.

Discussion

The outlined experimental findings confirm our previous observations on voltage bumps [17, 21] by more easily interpretable parameters of bump size and shape. They can all be explained plausibly in terms of our model of bump generation. Our

more detailed study of the bump latency distributions again confirms former observations that bump latency and bump *properties* are controlled by distinctly different processes. Several experimental variations influence the bump (size and shape) and its latency differently:

a) Latency and bump size (amplitude or current-integral) are not correlated at a constant state of adaptation [17, 24, 25, 38, 39, 41, 42].

b) Latency and slope of bump rise are not correlated at a constant state of adaptation [24, 25].

c) Latency and bump size are influenced differently by the mutation *norp A* in *Drosophila* [43] and by the mutation *nss* in *Lucilia* [44].

d) The temperature dependence of the bump latency has a coefficient Q_{10} of about 4 as compared to about 2.5 for bump amplitude and duration [12, 38, 39].

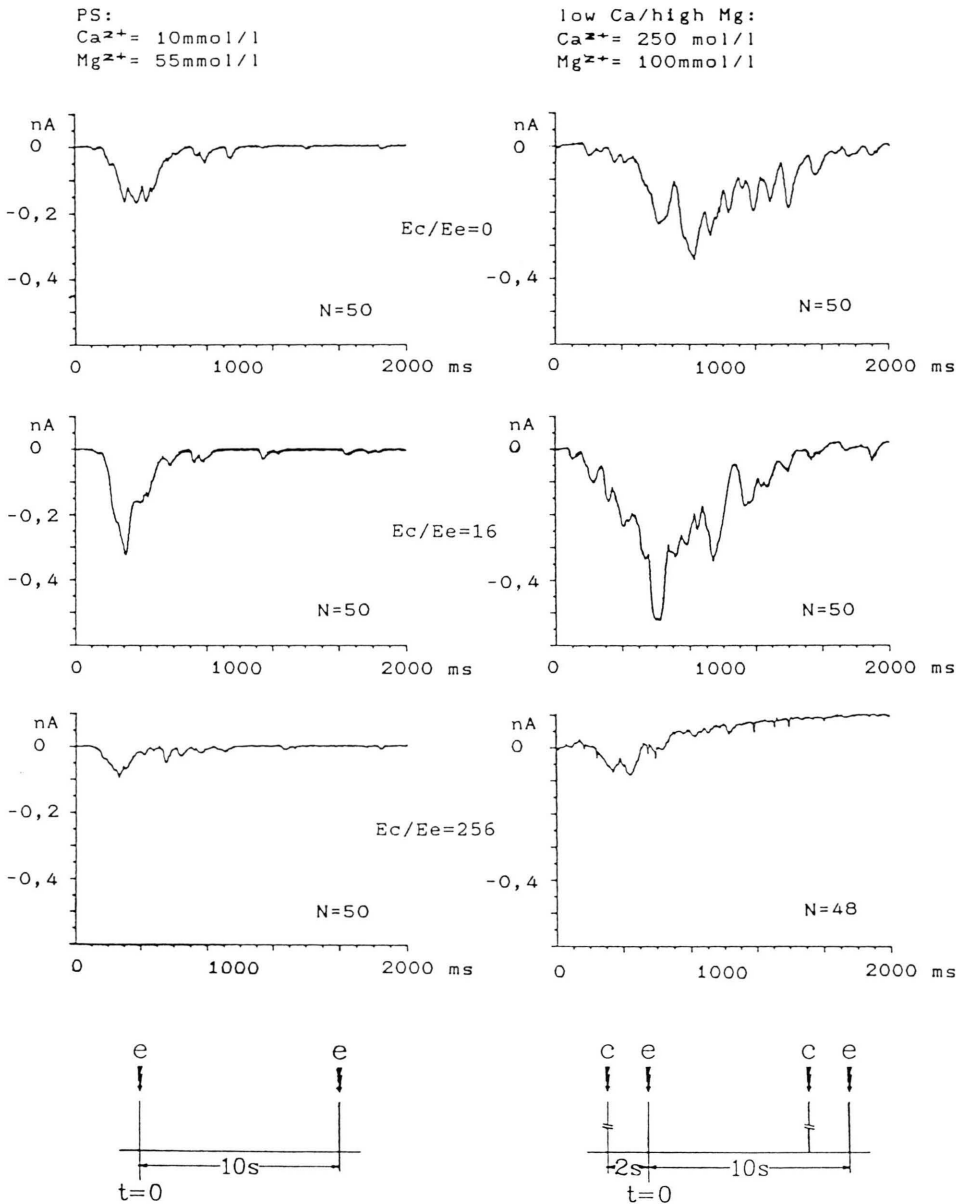


Fig. 14. Normalized bump sums. Summed bump responses to many very dim flashes in three different states of adaptation ($E_c/E_e = 0; 16; 256$). Left column: photoreceptor is superfused by physiological saline, right column: 25 min later the same photoreceptor superfused by a saline in which the calcium concentration was lowered to $250 \mu\text{mol/l}$ and magnesium concentration raised to 100 mmol/l . N: number of summed bump responses. KL090, further details as in Fig. 12.

e) Facilitation by a weak conditioning flash enhances the bump size and all other bump parameters opposite to the changes caused by light adaptation, whereas the bump latency is shortened as by light adaptation ([24] and present results).

f) Finally: raised external magnesium concentration partially substitutes for a lack of calcium; however, it enhances the prolonging effect of calcium deficiency on the latency (this study).

The bump, its time course and amplification,

seems not to “remember” the duration of the latency. Therefore we will discuss these response phenomena separately.

Action of calcium

Calcium influences many different processes in the *Limulus* photoreceptor cell [46]. Only in some of them magnesium can partially replace calcium [35, 47].

Calcium is a well known intracellular transmitter for light adaptation (for summary see [48–50]). The light-induced rise in intracellular calcium concentration causes, *via* a negative feedback loop, a graded desensitization of the photoreceptor cell. It even acts back on itself by reducing the further IP₃-mediated calcium release from intracellular stores [51]. The site of this action of calcium is intracellular. There are also actions of calcium on the extracellular surface of the cell membrane, concerning electrical screening effects and probably the site of the sodium/calcium-binding competition [35, 47].

If the external calcium concentration is lowered to 250 µmol/l the shift in sensitivity caused by strong pre-illumination is much diminished. Raising the external calcium has the opposite effect [26, 52].

Changing the external calcium concentration affects the intracellular, cytosolic calcium concentration which under physiological conditions is below 5 µM in the dark-adapted photoreceptor cell [53–55]. O'Day and Gray-Keller [55] and Deckert and Stieve [56] have shown that, due to the sodium/calcium exchange across the cell membrane, the extracellular calcium concentration strongly influences the cytosolic calcium concentration. However, the intracellular calcium stores, the subrhabdomeral cisternae (SRC), are not emptied if the extracellular calcium concentration is lowered, unless the cell is repeatedly stimulated by bright light [57].

The action of magnesium is in part extracellular. Magnesium is a substitute in the sodium/calcium-binding competition [35]. The sites of the other actions of magnesium on the light response are not known. In the vertebrate rod outer segment magnesium is not a substitute for calcium in the sodium/calcium exchanger [58] but it may be able to penetrate the cell membrane [59, 60]. The intracellular magnesium concentration is only a few

mmol/l (1.7 mmol/l measured in *Balanus* photoreceptor [61] and 3.0–3.5 mmol/l in squid axons [62]).

The magnesium effect in the experiments described here is somewhat surprising. An only two-fold rise in magnesium has a strong augmenting effect on the prolongation of the latency due to lowering of calcium. This confirms and expands our former proposition derived from macroscopic receptor potentials [22] by direct observation of individual bump latencies: The effect of calcium deficiency on the bump latency distribution is not antagonized but rather increased by a raise in external magnesium. This action of magnesium may be due to a competitive binding of magnesium to calcium-binding sites with no or only a weak effect. Magnesium seems not to desensitize the cell as much as calcium and therefore does not much change the bump except for a slight diminution of the bump size.

The molecular mechanism of the calcium action on the amplification in light and dark adaptation is unknown [51]. In terms of our model calcium might control the amplification by desensitizing the channel molecules or by regulating the activity of the source Q and thereby controlling the amount of active transmitter produced per bump. It could achieve the latter either by inhibiting the transmitter production or by accelerating the transmitter decay. It seems probable that calcium changes the activity of an enzyme by binding to a protein and inducing protein phosphorylation. Wiebe *et al.* [63] described a 46 kDa protein which upon illumination is phosphorylated *via* a Ca/calmodulin-dependent protein kinase.

The effect of calcium deficiency on the dark-adapted photoreceptor

The changes in the bump response of the photoreceptor due to lowering the external calcium in our experiments are most pronounced in the dark-adapted photoreceptor. Lowering of the external calcium concentration seems to act like an “extra” dark adaptation by increasing bump latency and bump size. However, facilitation and light adaptation are not much affected by this calcium deficiency.

A suggestive explanation is that the calcium concentration in the cytosol of the photoreceptor

cell is lowered due to the lowered extracellular calcium concentration *via* the Na/Ca exchanger in the plasma membrane. If the external calcium concentration is lowered the exchanger should export calcium and lower the cytosolic calcium concentration to reach an equilibrium for calcium gradient, sodium gradient and voltage across the plasma membrane [56]. However, the calcium content of the subrhabdomeral cisternae SRC is not much lowered since the cell is only weakly illuminated [57]. Thus weak light adaptation can still evoke an almost unchanged calcium release from the cisternae and the level of cytosolic Ca^{2+} concentration rises transiently as under physiological conditions. The ability for weak light adaptation remains almost unimpaired.

The observed changes in the bump due to lowering external calcium are dominated by an increase in the bump amplitude. The observed increase in bump width and bump rise time may be due entirely – or at least to a great part – to the increase in bump size. With increasing amplitude, if everything else is unchanged, the width of the bump should be increased proportional to the amplitude. Moreover, if the bumps are larger, more of them exceed the noise level; this can account for some increase in bump frequency.

In terms of our model the bump size may be increased because the source Q produces more transmitter. This could also be the explanation for the observed increase in the bump number: If the transmitter-gated channels must have bound 4 or 5 transmitter molecules in order to open, a certain number of rhodopsin activations will fail to lead to the formation of enough transmitter in the bump speck to open the necessary number of channels for a bump above the noise level. There may even be an unknown number of hidden bump specks in which the transmitter concentration is so small that not a single channel is opened.

The number of bumps exceeding the noise level will be raised (both for light-evoked and spontaneous bumps) if the average number of transmitter molecules per activated source Q is raised. This effect which might explain the observed rise in bump number due to lowered calcium should depend on the noise level and therefore vary from cell to cell.

It therefore seems plausible to us that all the observed effects of lowered external calcium in the dark-adapted photoreceptor on the bump proper-

ties and the increase in bump number might be explained alone by an “extra” dark adaptation which causes an increase in the production of transmitter. These changes in the bump are not much influenced when magnesium is raised.

Calcium seems to have a direct influence on the processes determining the latency which is independent of its action on amplification (bump size). This is indicated by the antagonistic effect of magnesium on the latency as compared to calcium – in contrast to the synergistic influence on all other bump parameters regarded. The reaction chain which determines the bump latency is very calcium-sensitive, it is accelerated by calcium and slowed down by magnesium.

Light adaptation

However, weak light adaptation – characterized by diminution of bump size – is in our experiments not much influenced by changes in external calcium or magnesium, a finding confirming former observations on voltage bumps [17]. This is in contrast to the fact that stronger light adaptation is much modified by changes in the external calcium concentration [24, 64, 65].

We proposed above that under our experimental conditions external calcium deficiency leads only to a decrease in cytosolic calcium, but the intracellular calcium stores (SRC) are not substantially exhausted. Due to the conditioning pre-illumination calcium would be released from these stores, causing an increase in intracellular calcium to about the same level as under physiological conditions. In terms of our model the raised calcium level would cause a reduction in the amount of released or active transmitter, *e.g.* by reducing the activity of the source Q. A negative feedback control by calcium on the release of the intracellular transmitter calcium was shown by Payne *et al.* [51]. This assumption can explain the observed desensitization in our experiments. The reduced transmitter release need not cause a lowering of the bump probability – as observed – if, due to the conditioning pre-illumination, some transmitter molecules are already bound to the light-activated channels previously to the bump-evoking flash.

Facilitation

In the *Limulus* photoreceptor under our experimental conditions facilitation – characterized by

increased bump number and/or size is also not much dependent of external calcium or magnesium but for a different reason as compared to light adaptation:

Facilitation is caused by very weak conditioning pre-illumination ($E_c/E_e < 16$) of a dark-adapted photoreceptor. Since facilitation and calcium reduction have the same effect on the bump size and shape but an opposite effect on the bump latency this is an argument against the assumption that facilitation is controlled by calcium. The underlying mechanism of facilitation may be, in terms of our model, that the conditioning pre-illumination causes a release of transmitter which, besides causing channel openings, binds to many channels below the threshold of opening. So the transmitter release induced by the following bump-evoking flash has a greater effect since a smaller number of additional transmitter molecules have to be bound in order to cause channel opening (as proposed by Reuß [66], Stieve [24] and Stieve and Schlösser [27]). The increase in bump number observed with facilitation could also be caused by channel preloading with transmitter since a smaller number of transmitter molecules is needed in order to open enough preloaded channels to exceed the noise level of recognition.

It is remarkable that the transition in the action of the pre-illumination from facilitation for weak pre-illumination to desensitization for stronger pre-illuminations ($E_c/E_e = 16$) seems not to depend much on the external calcium concentration. We suspect that it depends primarily on the number of channels pre-affected by transmitter.

However, stronger calcium deprivation may influence facilitation: Bolsover and Brown [57] described a so-called "calcium-deprived state" of the *Limulus* photoreceptor after prolonged stay in low external calcium concentration and frequent light stimulation. Under these conditions injection of calcium raises the sensitivity of the cell. Under similar conditions we have measured the stimulus dependence of the macroscopic response for two states of adaptation: 10–20 s (light-adapted) and 120 s (dark-adapted) after a strong conditioning illumination [26, 67]. We have found that the shift in sensitivity due to light adaptation was abolished in calcium-deficient saline. However, the two response characteristics intersected, displaying the following effect: Stimulation with small intensities

evokes small responses which are larger in the light-adapted than in the dark-adapted state, whereas stimulation by stronger stimuli causes responses which are – as normal – larger in the dark-adapted state. This is the same phenomenon as facilitation which is always observed for low stimulus intensities only. In the calcium-deprived state facilitation seems to be stronger or longer lasting than under normal conditions resulting in the observed response augmentation due to light adaptation. Light-adapting illumination causes here an increase in sensitivity, according to our hypothesis due to preloading of channels with ligand transmitters while the concomitant desensitization is reduced. These findings can be explained by the assumption that in the calcium-deprived state the decay of the light-induced transmitter increase is much retarded. Many channels were still subthresholdly preloaded with bound transmitter when the test flash was administered 10–20 s after the conditioning illumination but not after 120 s.

The difference in the calcium dependence of facilitation in photoreceptors of *Limulus* and of *Balanus* [40] may be due to the more rapid exchange of calcium between bath and barnacle photoreceptor [68].

Facilitation and supralinearity

In former publications [24, 26, 27] we discussed the supralinear response characteristics of the *Limulus* photoreceptor. The response current-integral vs. stimulus intensity rises more steeply than proportional over a certain intensity range. This supralinearity indicates that the single photon-evoked events which constitute the macroscopic receptor current are not independent of each other. The supralinear slope results from some kind of positive cooperativity. The observed slope of up to four could be explained by at least four ligands which have to be bound by a channel molecule [24]. The supralinear slope starts at an energy of the light flash where about 10–30 rhodopsin molecules have been activated by photon absorption and it ends (changes into a sublinear slope) at roughly 100–200 light-activated rhodopsin molecules. Under the assumption that 4 or 5 ligand transmitter molecules have to be bound to open a channel, we explained the supralinear slope in terms of our model by the overlapping of the coronas of bump specks. These coronas have bound

not yet enough transmitter molecules to be opened, but are already "unlocked" [27]. If the dissociation of the bound transmitter from the channels is a slow process, supralinearity caused by simultaneous illumination could be based on the same phenomenon as facilitation caused by sequential illumination. Preloading of channels would then be the basis of both facilitation and supralinearity. The question is raised whether the very weak pre-illumination in our experiments is sufficient to explain the observed facilitation by channel preloading. In our experiments the weak bump-evoking flash evoked 2–3 bumps (Table III) corresponding to 2–3 light-activated rhodopsin molecules. Facilitation was evoked if E_c/E_e was between 0.06 and 16. That corresponds to 0.15 to 40 light-activated rhodopsin molecules per conditioning flash. Facilitation induced by such weak pre-illumination which evokes not even one bump per cycle can only be explained if the cell remembers the effect of pre-illumination for more than one cycle. The life time of the (unlocked) conditioned state must be rather long, probably several 10 s.

Excitation, facilitation and adaptation are not restricted to the site of photon absorption but spread over a relatively large region of the cell. The effects of photon absorption should "infect" at least one hundredth to one thirtieth of the total area of the photosensory membrane of the R-lobe or its functional background. The estimate wavers since we cannot say yet how long the facilitating effect takes to decay [27].

Grzywacz, Hillman and Knight [69], assuming bump independence, deduced from noise analysis of *Limulus* photoreceptor current responses to light flashes of various intensities that with increasing stimulus intensity in the supralinear range the calculated bump amplitude is raised, whereas the calculated bump width and number of bumps evoked by the flash are not much changed. We ob-

served, however, at much lower energy of the light flash where we still could directly observe and measure individual bumps that in facilitation, besides the amplitude, also bump width and number of light-evoked bumps were increased in ratios varying from cell to cell.

Additional explanation

Our explanation presented so far may be sufficient to cover all the effects described here. However, there seems to be an additional control mechanism of the sensitivity in adaptation as revealed by the second phase of dark adaptation [64, 70, 71] which is fairly insensitive to calcium and may possibly be controlled by cAMP [65].

Schlösser [72] and Schlösser and Stieve [65] showed that the number of bumps generated by dim illumination rises when the intracellular cAMP level of the *Limulus* photoreceptor is raised by dibutyryl cAMP, IBMX, or theophyllin.

Edwards *et al.* [73] described a 122 kDa protein which is phosphorylated either induced by light or by cyclic AMP. It may be that cyclic AMP influences additionally the observed facilitation and/or the observed weak calcium-independent desensitization.

Acknowledgements

We wish to thank B. Minke, K. Nagy, J. Schnakenberg and R. Stephenson for helpful comments on the manuscript and K. Nagy and J. Schnakenberg and his coworkers for stimulating discussions.

We are grateful to M. Bruns, H. Gaube, K. Nauss and I. Wicke for their trouble with the manuscript.

This work was supported by the Deutsche Forschungsgemeinschaft (SFB 160).

- [1] A. Borsellino and M. G. F. Fuortes, *J. Physiol.* **196**, 507–539 (1968).
- [2] S. Yeandle, *Am. J. Ophthalmol.* **46**, 82 (1958).
- [3] S. Yeandle and M. G. F. Fuortes, *J. Gen. Physiol.* **47**, 443–463 (1964).
- [4] W. Keiper, Dissertation, RWTH Aachen (1983).
- [5] F. Wong, *Nature* **276**, 76–79 (1978).
- [6] J. Bacigalupo and J. E. Lisman, *Nature* **304**, 268–270 (1983).
- [7] J. Bacigalupo and J. E. Lisman, *Biophys. Journal.* **45**, 3–5 (1984).
- [8] J. Bacigalupo, K. Chinn, and J. E. Lisman, *J. Gen. Physiol.* **87**, 73–89 (1986).
- [9] K. Nagy and H. Stieve, *Eur. Biophys. J.* **18**, 221–224 (1990).
- [10] K. Nagy, *Eur. Biophys. J.* **19**, 47–54 (1990).
- [11] A. Adolph, *J. Gen. Physiol.* **48**, 297–322 (1964).
- [12] R. B. Srebro and M. Behbehani, *J. Physiol.* **224**, 349–361 (1972).

- [13] T. D. Lamb, *Vision Res.* **21**, 1773–1782 (1981).
- [14] J. E. Lisman, *J. Gen. Physiol.* **85**, 171–187 (1985).
- [15] S. Yeandle and J. B. Spiegler, *J. Gen. Physiol.* **61**, 552–572 (1973).
- [16] M. A. Goldring and J. E. Lisman, *IEEE Trans. SMC* **13**, 727–731 (1983).
- [17] H. Stieve and M. Bruns, *Biophys. Struct. Mech.* **9**, 329–339 (1983).
- [18] R. Lederhofer, Ph.D. thesis, RWTH Aachen (1989).
- [19] R. Lederhofer, J. Schnakenberg, and H. Stieve, *Z. Naturforsch.* **46c**, 291–304 (1991).
- [20] H. Stieve, in: *Information and Energy Transduction in Biological Membranes*, pp. 313–324, A. R. Liss Inc., New York 1984.
- [21] H. Stieve and M. Bruns, *Biophys. Struct. Mech.* **6**, 271–285 (1980).
- [22] H. Stieve, M. Bruns, and H. Gaube, *Z. Naturforsch.* **38c**, 471–483 (1983).
- [23] H. Stieve, in: *Neurobiology* (R. Gilles and J. Balthazart, eds.), pp. 346–362, Springer Verlag, Berlin, Heidelberg 1985.
- [24] H. Stieve, in: *The Molecular Mechanism of Photoreception* (H. Stieve, ed.), pp. 199–230, Dahlem-Konferenzen, Springer Verlag, Berlin, Heidelberg, New York, Tokio 1986.
- [25] W. Keiper, J. Schnakenberg, and H. Stieve, *Z. Naturforsch.* **39c**, 781–790 (1984).
- [26] H. Stieve, H. Gaube, and J. Klomfaß, *Z. Naturforsch.* **41c**, 1092–1110 (1986).
- [27] H. Stieve and B. Schlösser, *Z. Naturforsch.* **44c**, 999–1014 (1989).
- [28] E. C. Johnson, P. R. Robinson, and J. E. Lisman, *Nature* **324**, 468–470 (1986).
- [29] R. Payne, D. W. Corson, A. Fein, and M. Berridge, *J. Gen. Physiol.* **88**, 127–142 (1986).
- [30] J. E. Brown and J. Coles, *J. Physiol.* **296**, 373–392 (1979).
- [31] C. Feng, Y. Xia, W. Pappas, and R. Stephenson, *J. Gen. Physiol.*, in print (1990).
- [32] H. Kühn, *Progress in Retinal Research* **3** (N. Osborne and J. Chader, eds.), 123–156 (1984).
- [33] M. Chabre and M. L. Applebury, in: *The Molecular Mechanism of Photoreception* (H. Stieve, ed.), pp. 51–66, Dahlem-Konferenzen 1986.
- [34] G. Dirnberger, W. Keiper, J. Schnakenberg, and H. Stieve, *J. Membr. Biol.* **83**, 39–43 (1985).
- [35] H. Stieve, M. Pflaum, J. Klomfaß and H. Gaube, *Z. Naturforsch.* **40c**, 278–291 (1985).
- [36] M. A. Goldring, Ph.D. thesis, Brandeis University (1982).
- [37] N. M. Grzywacz and P. Hillman, *Proc. Natl. Acad. Sci. U.S.-Biol. Sci.* **82**, 232–235 (1985).
- [38] F. Wong, B. W. Knight, and F. A. Dodge, *J. Gen. Physiol.* **76**, 517–537 (1980).
- [39] J. Howard, *Biophys. Struct. Mech.* **9**, 341–348 (1983).
- [40] M. P. Hanani and P. Hillman, *The Journal of General Physiol.* **67**, 235–249 (1976).
- [41] J. Schnakenberg and W. Keiper, in: *The Molecular Mechanism of Photoreception* (H. Stieve, ed.), pp. 353–367, Dahlem-Konferenzen, Springer Verlag, Berlin, Heidelberg, New York, Tokio 1986.
- [42] J. Schnakenberg, *Biol. Cybern.* **60**, 421–437 (1989).
- [43] W. L. Pak, S. E. Ostroy, M. C. Deland, and C. F. Wu, *Science* **194**, 956–959 (1976).
- [44] S. Barash, E. Suss, D. G. Stavenga, C. T. Rubinstein, Z. Selinger, and B. Minke, *J. Gen. Physiol.* **92**, 307–330 (1988).
- [45] A. Adolph, *J. Gen. Physiol.* **52**, 584–599 (1968).
- [46] H. Stieve, in: *Sense Organs* (M. S. Laverack and D. J. Cosens, eds.), pp. 163–185, Blackie and Son Ltd., Glasgow, London 1981.
- [47] H. Stieve and M. Bruns, *Z. Naturforsch.* **33c**, 574–579 (1978).
- [48] J. E. Brown, in: *The Molecular Mechanism of Photoreception* (H. Stieve, ed.), pp. 231–240, Dahlem-Konferenzen 1986.
- [49] J. E. Lisman and J. E. Brown, *J. Gen. Physiol.* **59**, 701–719 (1972).
- [50] J. E. Lisman and J. E. Brown, *J. Gen. Physiol.* **66**, 489–506 (1975).
- [51] R. Payne, T. M. Flores, and A. Fein, *Neuron* **4**, 547–555 (1990).
- [52] H. Stieve, M. Bruns, and H. Gaube, *Z. Naturforsch.* **39c**, 662–679 (1984).
- [53] J. E. Brown, P. K. Brown, and L. H. Pinto, *J. Physiol.* **267**, 299–320 (1977).
- [54] S. Levy and A. Fein, *J. Gen. Physiol.* **85**, 805–841 (1985).
- [55] P. M. O'Day and M. P. Gray-Keller, *J. Gen. Physiol.* **93**, 473–492 (1989).
- [56] A. Deckert and H. Stieve, *J. Physiol. (London)* **433**, 467–482 (1990).
- [57] S. R. Bolsover and J. E. Brown, *J. Physiol.* **346**, 381–393 (1985).
- [58] K. W. Yau and K. Nakatani, *Nature* **311**, 661–663 (1984).
- [59] K. Nakatani and K. W. Yau, *Biophys. J.* **51**, 18a (1987).
- [60] K. W. Yau and K. Nakatani, *J. of Physiol.* **395**, 695–729 (1988).
- [61] B. Rydqvist and H. M. Brown, *Acta Physiol. Scand.* **127**, 499–506 (1986).
- [62] F. J. Brinley and A. Scarpa, *FEBS Lett.* **50**, 82–85 (1975).
- [63] E. M. Wiebe, A. C. Wishart, S. C. Edwards, and B.-A. Battelle, *Visual Neuroscience* **3**, 107–118 (1989).
- [64] I. Claßen-Linke and H. Stieve, *Z. Naturforsch.* **41c**, 657–667 (1986).
- [65] B. Schlösser and H. Stieve, in: *Dynamics and Plasticity in Neuronal Systems* (N. Elsner and W. Singer, eds.), Georg Thieme Verlag, Stuttgart, New York 1989.
- [66] H. Reuß, Diplomarbeit, RWTH Aachen (1985).
- [67] H. Stieve and M. Pflaum, *Vision Res.* **18**, 747–749 (1978).
- [68] J. E. Brown, J. R. Blinks, *J. Gen. Physiol.* **64**, 643–665 (1974).
- [69] N. M. Grzywacz, P. Hillman, and B. W. Knight, *J. Gen. Physiol.* **91**, 659–684 (1988).
- [70] G. Maaz, K. Nagy, H. Stieve, and J. Klomfaß, *J. Comp. Physiol.* **141**, 303–310 (1981).
- [71] K. Nagy and H. Stieve, *Biophys. Struct. Mech.* **9**, 207–223 (1983).
- [72] B. Schlösser, Ph.D. thesis, RWTH Aachen (1990).
- [73] S. C. Edwards, A. C. Wishart, E. M. Wiebe, and B.-A. Battelle, *Visual Neurosci.* **3**, 95–105 (1989).